Luminescent enhancement of ligand-centered photoluminescence in inorganic-organic frameworks for solid state lighting

Joshua D. Furman,[a,b] Brent C. Melot,[c] Simon J. Teat,[d] Alexander A. Mikhailovsky,[e] and Anthony K. Cheetham[*,a]

Contents

[a] University of Cambridge, Department of Materials and Metallurgy. Cambridge, UK, CB2 3QZ; E-mail: akc30@cam.ac.uk
[b] University of California Santa Barbara, Mitsubishi Chemical Center for Advanced Materials. Santa Barbara, CA, USA.
[c] University of California Santa Barbara, Materials Department, Santa Barbara, CA, USA.
[d] Lawrence Berkeley National Laboratory, Advanced Light Source, Berkeley, CA, USA.
[e] University of California Santa Barbara, Department of Chemistry, Santa Barbara, CA, USA.

1 Optical characterization

Room temperature photoluminescence measurements were carried out at room temperature using a Perkin Elmer LS55 fluorescence spectrometer. Temperature dependent emission spectra were collected using 405 nm laser excitation and a LN_2 cooled cryostat or resistive heating stage in combination with an Acton Research spectrometer.

Emission quantum yield (QY) measurements were performed on finely ground powder samples mounted in silicone resin on optical quartz substrates. A Labsphere integrating sphere with excitation light from a Spectraphysics Beamlock 2065 Ar-ion laser at 363 nm or 405 nm was used to illuminate the samples. The experimental setup is similar to the one described in a paper by Greenham et al [7]. The light exiting the sphere passed through appropriate coloured glass or interference filters. Emission was detected using a Newport UV-818 calibrated Si photodiode, amplified with a Stanford Research Systems SR570 and measured using a Keithley 195 digital multimeter.

1.1 Room temperature luminescence

The excitation curve of the parent ligand H_2FDC (Figure 1), measured at λ_{em}=500 nm, shows strong peaks near 390 nm and 440 nm and then decreases sharply. The accompanying emission curve, measured at λ_{ex}=440 nm, shows a broad emission centred at 515 nm. Room temperature excitation and emission curves of H_2FDC, CaFDC, SrFDC, BaFDC, and CdFDC show broad emission that is yellow for the ligand itself, and shifted slightly for each framework structure. MnFDC did not show visible photoluminescence, presumably due to the paramagnatism of the Mn^2+ cation. The excitation spectra for BaFDC (Figure 2), measured at λ_{em}=535 nm, peaks at 400 nm and 445 nm. The emission spectra, measured at λ_{ex}=365 nm, has a maximum at 517 nm. The excitation spectra for CdFDC (Figure 3), measured at λ_{em}=535 nm, peaks at 394 nm, 450 nm, 468 nm. The emission spectra, measured at λ_{ex}=365 nm, has a maximum at 428 nm. The excitation curve of CaFDC (Figure 4), measured under the same conditions, is mostly constant into the blue and drops sharply at 460 nm. The emission curve, measured at λ_{ex}=440 nm, peaks at 503 nm with a long tail into the red. Similarly, the excitation of SrFDC (Figure 5) drops sharply at 460 nm and the emission peaks at 526 nm.
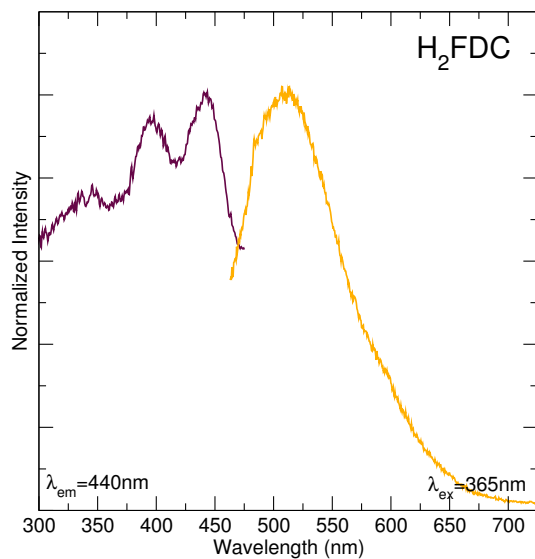
Figure 1 Photoluminescent excitation and emission spectra for the free ligand H$_2$FDC, $\lambda_{ex} =$ 440 nm, $\lambda_{em} =$ 500 nm.
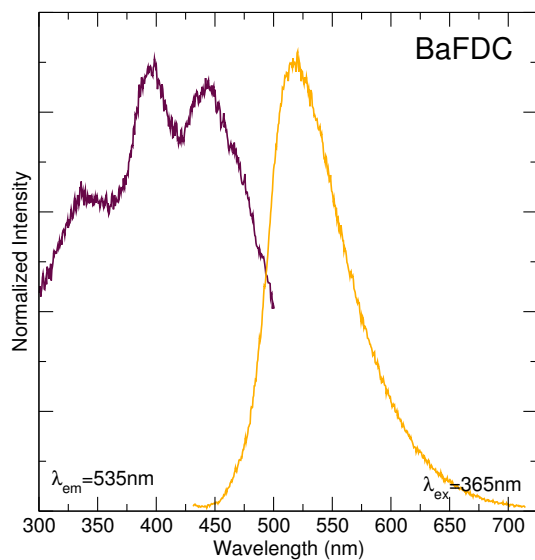
Figure 2 Photoluminescent excitation and emission spectra for BaFDC, $\lambda_{ex} =$ 365 nm, $\lambda_{em} =$ 535 nm.
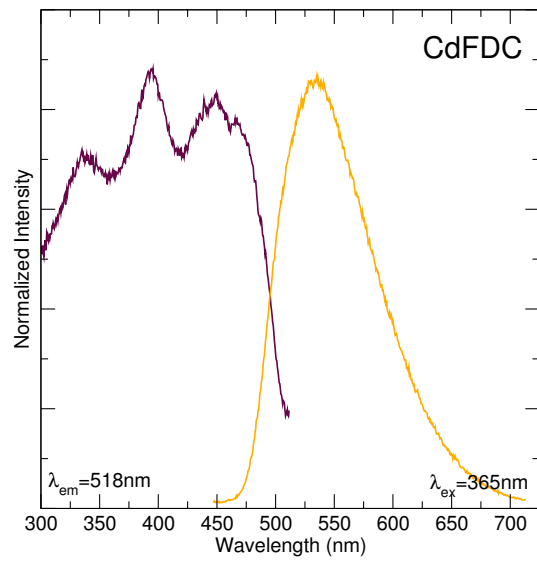
Figure 3 Photoluminescent excitation and emission spectra for CdFDC, λ_{ex} =365 nm, λ_{em} =535 nm.
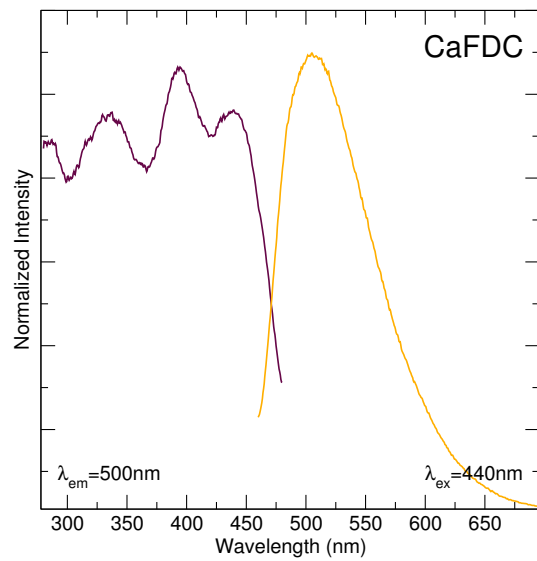
Figure 4 Photoluminescent excitation and emission spectra for CaFDC, λ_{ex} =440 nm, λ_{em} =500 nm.
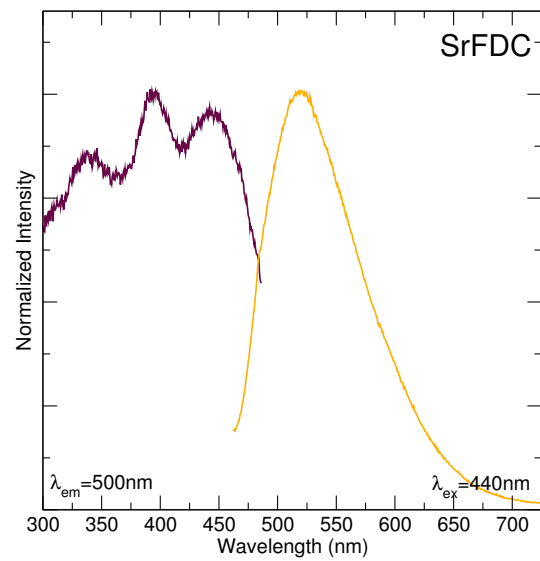
Figure 5 Photoluminescent excitation and emission spectra for SrFDC, λ_{ex} =440 nm, λ_{em} =500 nm.

1.2   Temperature dependent luminescence

Temperature dependent emission spectra for H_2FDC and the luminescent fluorenone frameworks are shown in Figures 6 through 8. Samples were all measured down to 77 K, although the maximum temperature varied slightly due to sample stability. An inverse-S type curve is expected for thermal quenching of luminescent states. H_2FDC and CaFDC exhibit this quite clearly, while the other compounds may but the decay occurs over a wider range than the compound is otherwise chemically stable.

The room temperature quantum yield (QY) of BaFDC was measured at 2.8%, CdFDC at 2.6%, CaFDC at 7.4%, SrFDC at 2.8%, and the ligand H_2FDC at 2.4%.
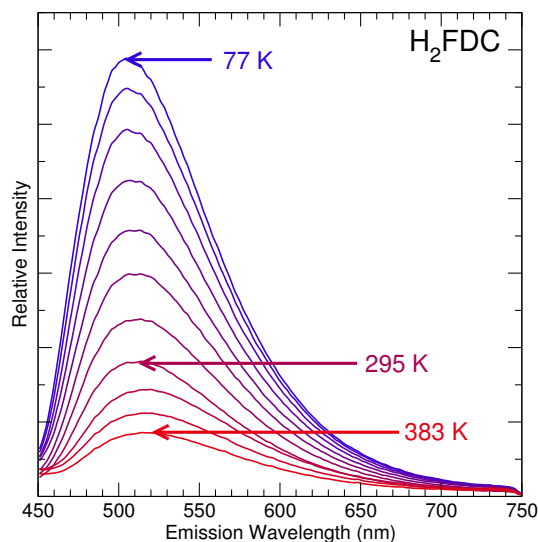
Figure 6 Temperature dependent emission spectra (λ_{ex} =405 nm) of H_2FDC, increasing in temperature from 77 K (blue) to 383 K (red).
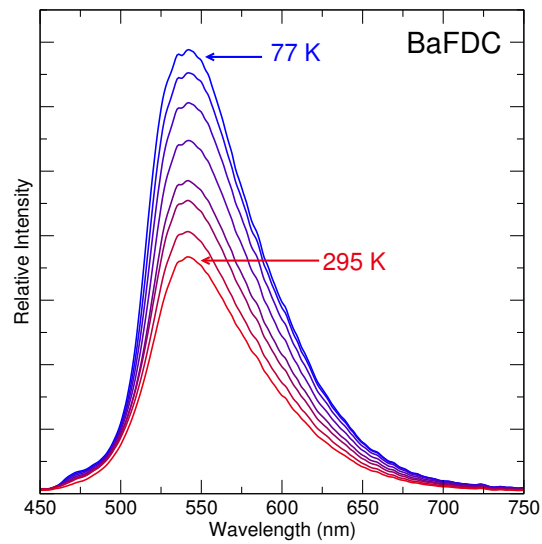
Figure 7 Temperature dependent emission spectra (λ_{ex} =405 nm) of BaFDC, increasing in temperature from 77 K (blue) to 295 K (red). High temperature data was omitted for clarity due to an emission colour shift.
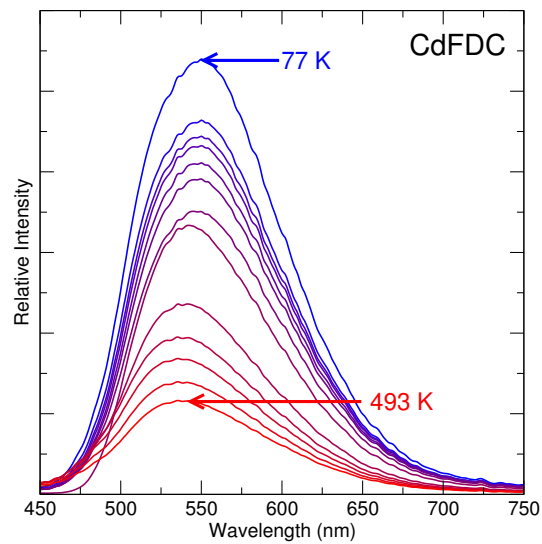
Figure 8 Temperature dependent emission spectra (λ_{ex} =405 nm) of CdFDC, increasing in temperature from 77 K (blue) to 493 K (red).
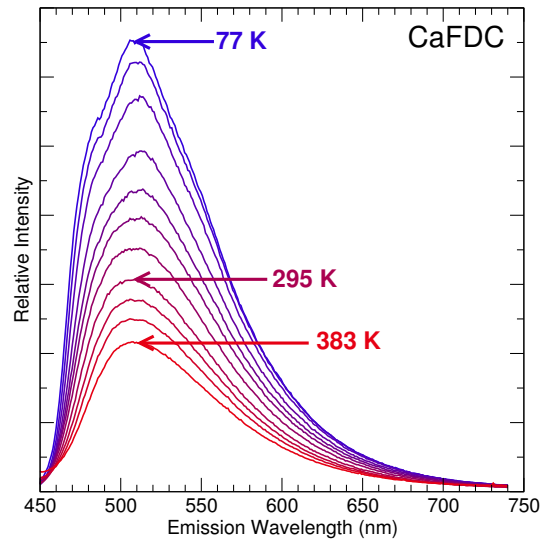
Figure 9 Temperature dependent emission spectra (λ_{ex} =405 nm) of CaFDC, increasing in temperature from 77 K (blue) to 383 K (red).
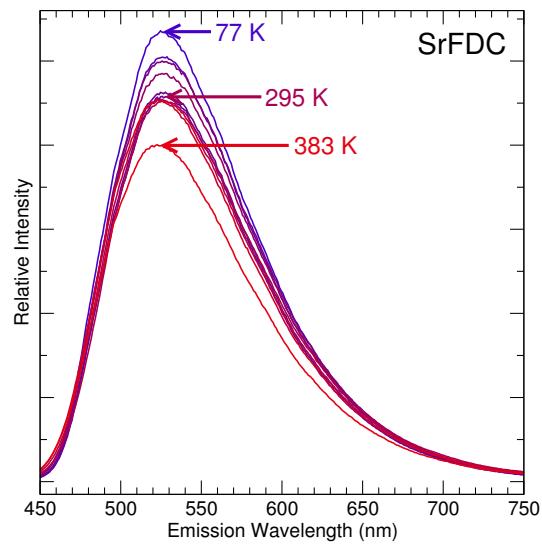
Figure 10 Temperature dependent emission spectra (λ_{ex} =405 nm) of SrFDC, increasing in temperature from 77 K (blue) to 383 K (red).

1.3 Time resolved luminescence

Fluorescence lifetime measurements were performed using the Time Correlated Single Photon Counting (TC-SPC) technique [8]. Excitation pulses of approximately 100 fs with a wavelength tunable from 360-470 nm were generated using a frequency doubling β-barium borate crystal in combination with a Spectra-Physics Tsunami mode-locked Ti-sapphire laser. The laser repetition rate was reduced to 2 MHz using an acousto-optical pulse picker to avoid chromophore saturation. The TCSPC system was equipped with a Hamamatsu R3809U-51 ultrafast microchannel plate photomultiplier tube detector and a Becker & Hickl SPC-630 counting module, providing a response time $\leq$50 ps. The triggering signal for the TCSPC board was generated by sending a fraction of the laser beam to a Si photodiode. The fluorescence spectrum was monitored using a Roper Scientific PIXIS-400B CCD camera equipped with an Acton Research SP300 monochromator and an ALP long-pass filter. Fluorescence transients were not deconvolved from the instrument response function since their characteristic time constants were much longer than the width of the system response to the excitation pulse. Variable temperature measurements were performed using a liquid nitrogen cryostat with temperature controller down to 77 K or a heating stage up to 500 K.

Time-resolved luminescence measurements allowed observation of the emission of the phosphor after a laser excitation pulse. When only one kind of process is involved, the emission intensity decreases mono-exponentially according to:

$$I_t = I_o e^{\frac{-t}{\tau}} \tag{1}$$

where I_t and I_o are the intensities of the emission at time t and at initial time t_o, respectively, and τ is the lifetime of the luminescence. The lifetime τ is the time when the population of the excited state has decreased to $\frac{1}{e}$ ($\sim$37%). If there is more than one process involved, the emission intensity can also decrease bi-exponentially according to:

$$I_t = I_1 e^{\frac{-t}{\tau_1}} + I_2 e^{\frac{-t}{\tau_2}} \tag{2}$$

where I_1 and I_2 are the intensities of the emissions of the different processes at t_o. τ_1 and τ_2 are the lifetimes of each process. Table 1 gives the exponential fit parameters for the fluorenone frameworks. For comparison, the decay constant for YAG:Ce is typically on the order of 50 nm, depending on the crystallinity of the sample [9, 10].

Table 1 Summary of luminescent lifetime decay exponentials for FDC compounds

Compound	I_1 (a.u.)	I_2 (a.u.)	τ_1 (ns)	τ_2 (ns)	$\frac{I_1}{I_2}$
BaFDC	4169	11854	7.2	2.0	0.35
CdFDC	8061	7138	11.7	2.8	1.13
CaFDC	10230	5339	11.4	3.3	1.92
SrFDC	10850	3820	12.4	4.3	2.84
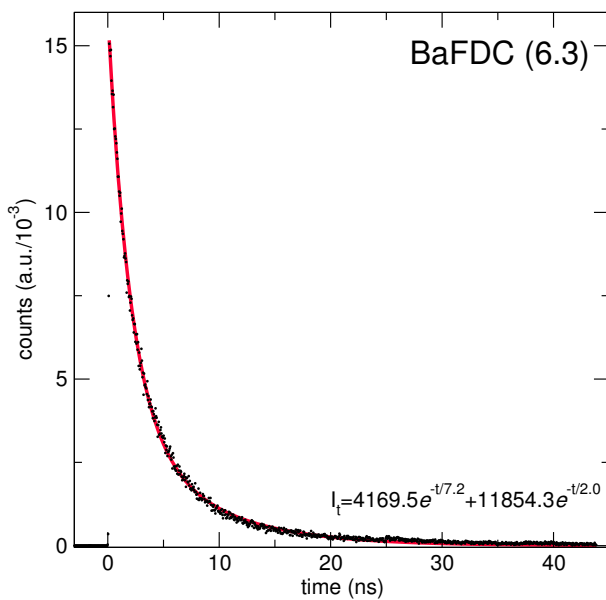
Figure 11 Luminescent lifetime of BaFDC. λ_{ex}=400 nm, λ_{em}=545 nm
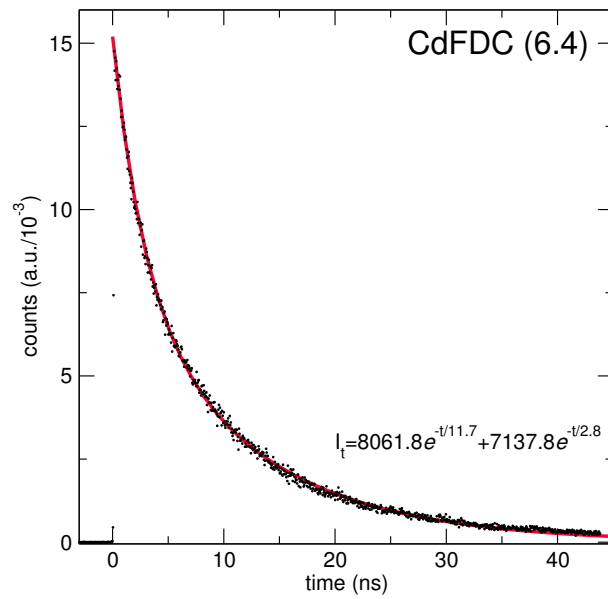
Figure 12 Luminescent lifetime of CdFDC. λ_{ex}=400 nm, λ_{em}=560 nm
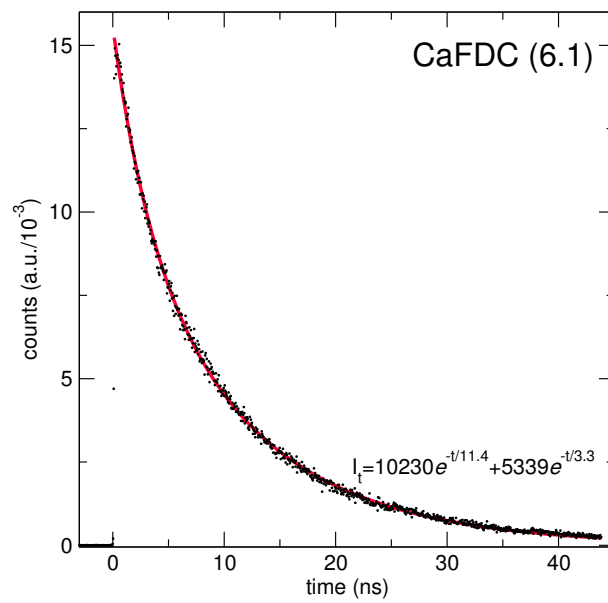
Figure 13 Luminescent lifetime of CaFDC. λ_{ex}=400 nm, λ_{em}=505 nm.

11
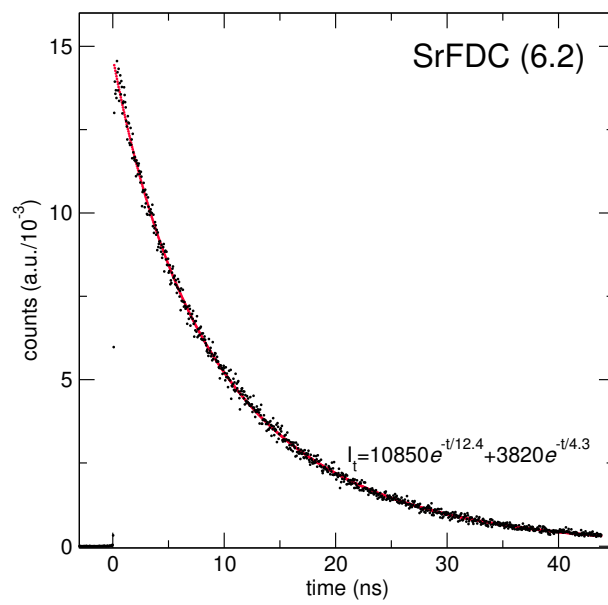
Figure 14 Luminescent lifetime of SrFDC. λ_{ex}=400 nm, λ_{em}=545 nm

2 Specific heat measurements

2.1 Methods

In addition to standard structural and optical characterization, specific heat measurements were carried out to evaluate vibrational modes in the materials as an attempt to explain differences in quantum yield between the compounds. Measurements of the fluorenone compound heat capacities were carried out on a Quantum Design Physical Properties Measurement System (PPMS) using a 2-τ relaxation technique [1]. Powder samples were mixed 1:1 by weight with silver powder, finely ground, and cold pressed into rectangular pellets which were then cut down to approximately $3\,\text{mm}\times3\,\text{mm}\times0.5\,\text{mm}$. The addition of the silver raises the thermal conductivity of the overall sample, increasing sensitivity [2]. Pellets are attached to a calorimeter using the thermally conductive Apiezon N grease. The contribution to the specific heat from the silver and grease are measured separately and subtracted. The sample holder contains both a resistance heater and a thermocouple. A power pulse is delivered to the heater for a fixed amount of time and the temperature change caused by delivering that heat to the sample is measured. The system temperature is lowered and allowed to stabilize between pulses, in this case from $80\,\text{K}$ down to $2\,\text{K}$. The behaviour of the temperature relaxation and contributions from the instrument are modelled internally and converted to specific heat.

2.2 Theory of specific heat measurements

Specific heat relates the total energy of a system (U) to the temperature (T) by:

$$\frac{\partial U}{\partial T} = \int C_p dT \tag{3}$$

It is related to the extrinsic property of heat capacity, the amount of heat needed to raise the temperature of a material by some amount. The specific heat is sensitive to changes in pressure, volume, magnetic field, and others, and so experimentally these parameters are selectively held constant and a value is often reported as the heat capacity at constant pressure C_p or at constant volume C_v in units of J·mol^{-1}·K^{-1}.

The partition function Z in statistical mechanics encodes how probabilities are divided, or partitioned, between microstates of a system:

$$Z = \sum_i e^{\frac{-\epsilon_i}{k_B T}} \tag{4}$$

where i are all the states of a system and ϵ_i is the energy at that state. This allows the rotational, electronic, magnetic, and lattice contributions to Z to be separated such that:

$$Z = Z_{rotation} \cdot Z_{electronic} \cdot Z_{magnetic} \cdot Z_{lattice} \tag{5}$$

And when combined with Equation 3 above, it is found that:

$$C_v = C_{v,rotation} + C_{v,electronic} + C_{v,magnetic} + C_{v,lattice} \tag{6}$$

Thus contributions to the specific heat by individual processes can be simply subtracted out of the total value. This is particularly useful in measurements, where the contribution of a sample holder or thermal grease can be removed as a baseline.

In 1819, Dulong and Petit introduced a rule stating that all solid elements at room temperature have the molar heat capacity $3R$, or 24.9 J·K^{-1}. This can be derived using classical oscillators with energy $k_B T$, moving with 3 degrees of freedom. However, an understanding the relationship of specific heat to temperature was not clear until the application of quantum theory [3]. The 1907 Einstein model treated each atom in a lattice as a single harmonic oscillator with quantized frequencies. This models the energy as localized vibrations rather than collective phonon vibrations. These vibrations can exist down to low temperatures, whereas classical collective modes cannot [4]. Thus the total energy in a system U can be derived as the sum of the quantized oscillators:

$$U_{\text{tot}} = 3 \sum_i n_i \left(i + \frac{1}{2} \right) h\nu \tag{7}$$

where i is the ith energy level, n_i is the number of moles, h is Plank's constant and the multiplier 3 arises from the three degrees of freedom in the x, y, and z directions. Extracting the heat capacity from this total energy approximation gives a relatively good match to measured values, approaching Dulong-Petit behaviour at high temperature and decreasing to 0 at 0 K. There was still, however, a slight mismatch between empirical data and the theoretical model at low temperatures.

Debye further refined Einstein's approach by constraining the range of frequencies available to the oscillators. The upper limit is set by the interatomic distances and the distribution increases parabolically per unit volume. This refinement of the model gives a very close fit to empirical data for many well behaved systems,

and more closely follows the increase in specific heat with temperature than the Einstein model, as shown in Figure 15. The characteristic Debye temperature, θ_D, indicates the cross-over point from low temperature quantized behaviour, where the atoms vibrate independently, to the high temperature classical region, where vibrations are coupled through the lattice. The Debye frequency ω_D is given as:

$$\omega_D = \left(\frac{6\pi^2 sN}{V}\right)^{1/3} \left(\frac{1}{c_L^3} + \frac{1}{c_T^3}\right)^{-1/3} \tag{8}$$

where s is the number of atoms per formula unit, N is the number of molecules per mole, V is the volume of the crystal, and c_L and c_T are the velocities of the longitudinal and transverse phonons [5]. This relates to the debye temperature θ_D by:

$$\theta_D = \frac{\hbar\omega_D}{k_B} \tag{9}$$

The specific heat then follows the function:

$$C_v = 9Rs\left(\frac{T}{\theta_D}\right)^3 \int_0^{x_D} \frac{x^4 e^x \, dx}{(e^x - 1)^2} \tag{10}$$

where:

$$x = \frac{\hbar\omega}{k_b T} \tag{11}$$

$$x_D = \frac{\hbar\omega_D}{k_b T} \tag{12}$$

In practice, the integral in Equation 10 is approximated by an odd-series taylor expansion such that:

$$C_v = \beta_3 T^3 + \beta_5 T^5 + \beta_7 T^7 \ldots \tag{13}$$

The cubic term of that expansion, β_3, can be used to extract the Debye temperature from the low temperature limit of the integral above, such that:

$$C_v = \frac{12\pi^4}{5}\left(\frac{Rs}{\theta_D^3}\right) T^3 = \beta_3 T^3 \tag{14}$$

$$\theta_D = \left(\frac{12\pi^4}{5}\frac{Rs}{\beta_3}\right)^{1/3} \tag{15}$$

The specific heat decreases sharply at low temperature as individual degrees of freedom are effectively "frozen" out of the vibration modes available to the atoms. While we are not considering the luminescence of materials at these low temperatures, the behaviour of the phonons provides insight into lattice dynamics at all temperatures.
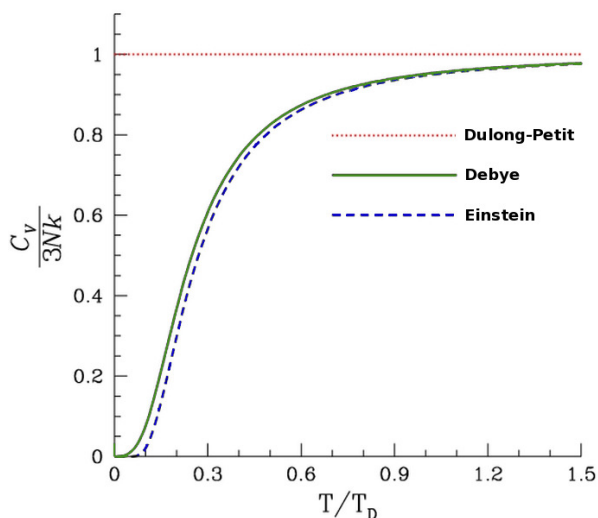
Figure 15 Specific heat as described by the Dulong-Petit law (dotted red), Debye model (green), and Einstein model (dashed blue), showing convergence at high temperature. The Einstein model deviates from the expected behaviour shown in the Debye model at low temperatures [3].

2.3 Results

The specific heat, as measured, is shown in Figure 16 and the calculations to extract the characteristic Debye temperatures are shown in Figure 17. They are summarized in Table 2, which lists the coefficients for fitting of Equation 10 to a 4 term taylor expansion, as described in Section 2.2. The data for H_2FDC is anomalous and has been omitted. This is not unexpected as the work of Talon et al. showed a large deviation from expected Debye behaviour for molecular solids as compared to amorphous and crystalline extended network solids. The behaviour of the fluorenone-containing frameworks shows no sharp peaks or discontinuities that would indicate a first or second order phase transition. They do all show a broad peak at around 10 K. The increased value of C_p/T^3 at low temperature for BaFDC as compared to the calcium-containing framework suggests that increased collective vibrations present in the lattice may be quenching the luminescent processes

by providing non-radiative recombination pathways as compared to the more localized vibrations in CaFDC. Similarly, the work of Ramos et al. showed higher values in the C_p/T^3 curves for glasses as compared to crystalline solids of the same composition [6]. Furthermore, the lowest Debye temperature in the framework structures was extracted for BaFDC, suggesting a lower temperature crossover to collective vibrations in the lattice. This may explain why, despite the broad structural and chemical similarity of the BaFDC and CaFDC samples, the luminescence of the barium compound is so reduced.

Table 2 Summary of fitting functions for heat capacity data with formula $AT + BT^3 + CT^5 + DT^7$ and Debye temperature θ_D

Compound	A/T	B/T^3	C/T^5	D/T^7	θ_D
H_2FDC	0.0268584	0.00479257	-2.39301e-5	7.57669e-8	225 K
BaFDC	0	0.00612649	-5.428e-6	-2.67416e-9	267 K
CdFDC	0	0.0261431	1.17412e-6	-1.42275e-8	299 K
CaFDC	0	0.00189032	-1.08458e-6	9.13224e-9	324 K
SrFDC	0	0.00262637	2.00472e-7	-8.61947e-9	381 K
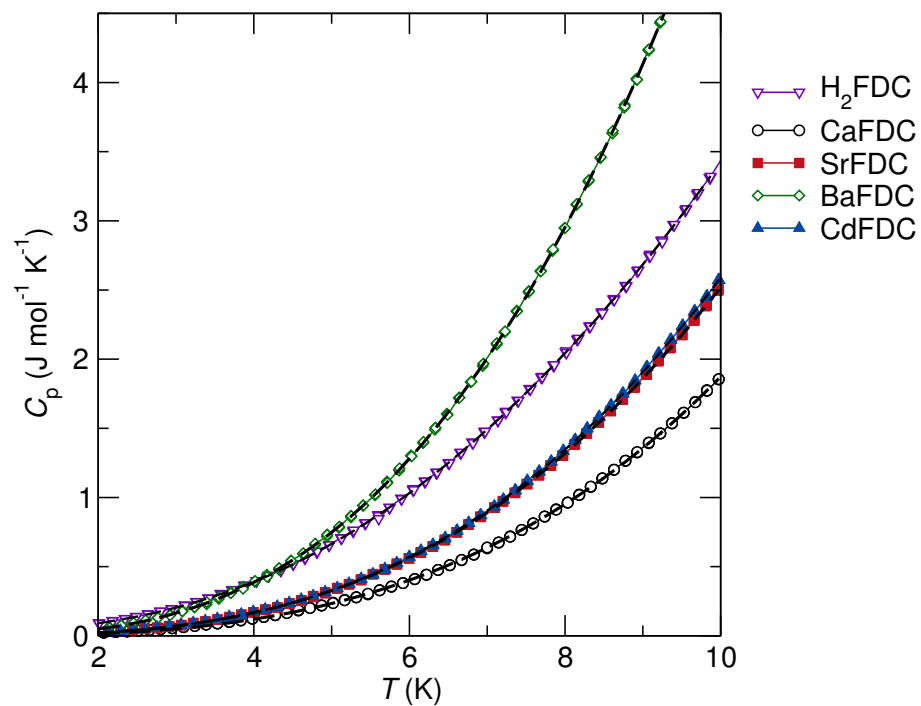
Figure 16 Heat capacity of ligand H_2FDC and fluorenone frameworks.
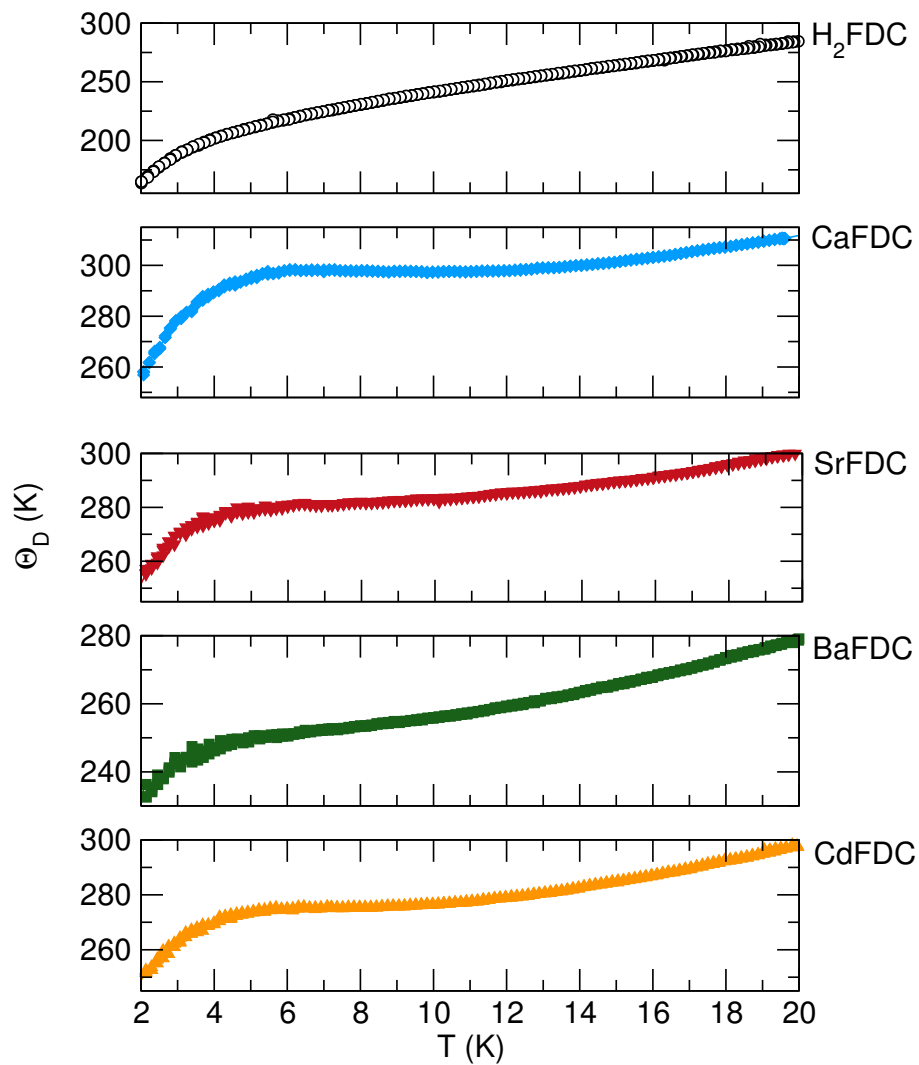
Figure 17 Debye temperature for the ligand H_2FDC and fluorenone frameworks.

3   Thermogravimetric analysis

Thermogravimetric analysis (TGA) was carried out in air for the fluorenone samples up to 1000°C, at which point they decomposed to their constituent oxides or carbonates, depending on the metal species. Data were collected using a Mettler 851e, with samples loaded in alumina crucibles and the temperature ramping at 10°C per minute. The decomposition products are summarized in Table 3. BaFDC (Figure 19) shows multiple small dehydration steps corresponding to a loss of 1 water molecule, followed by a large weight loss step starting at 430°C and ending at 557°C, where the compound decomposes to barium carbonate. CdFDC (Figure 20) shows dehydration steps up to 150°C corresponding to the loss of 3 water molecules, as expected from the formula, and then a large weight loss starting at 350°C and ending at 500°C where the compound decomposes to cadmium oxide. MnFDC (Figure 21) shows a dehydration step between 120°C and 220°C corresponding to a loss of two water molecules, followed by decomposition and oxidation to manganese dioxide between 420°C and 510°C. Thermal gravimetric analysis in air of CaFDC (Figure 22) shows removal of the two water molecules in two steps near 115°C and 200°C. An anhydrous phase is then present on heating until 560°C, where the compound decomposes to calcium carbonate and then finally to calcium oxide at 713°C. Analysis of SrFDC (Figure 23) shows dehydration steps ending at at 127°C and 270°C corresponding to a loss of 3.5 water molecules to an anhydrous structure that is stable to 400°C. Decomposition to strontium carbonate is completed at 560°C, and a final decomposition to strontium oxide occurs between 800°C and 960°C.

Table 3 Thermogravimetric analysis of fluorenone frameworks

Compound	Initial Mass (g·mol^{-1})	Final Mass Percent (%)	Observed final mass (g·mol^{-1})	Decomposition product	Ideal decomposition mass (g·mol^{-1})	Error (%)
BaFDC	421.55	43.2	182.3	BaCO$_3$	197.3	7.6
CdFDC	432.65	31.4	135.8	CdO	128.4	5.7
MnFDC	357.17	24.3	86.8	MnO$_2$	88.69	0.2
CaFDC	342.31	16.5	56.5	CaO$_2$	56.1	0.7
SrFDC	416.88	25.5	106.3	SrO	103.6	2.6
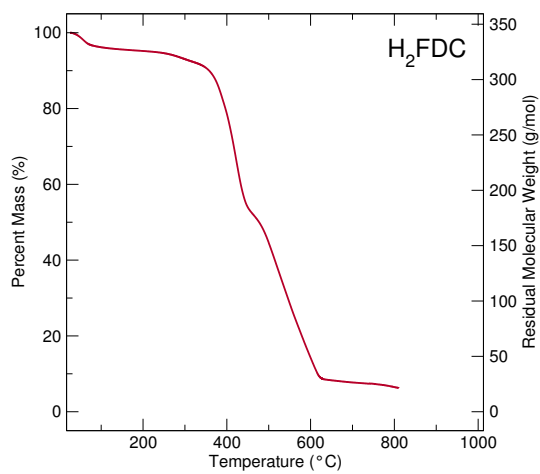
Figure 18 Thermogravimetric analysis of H$_2$FDC in air.

21
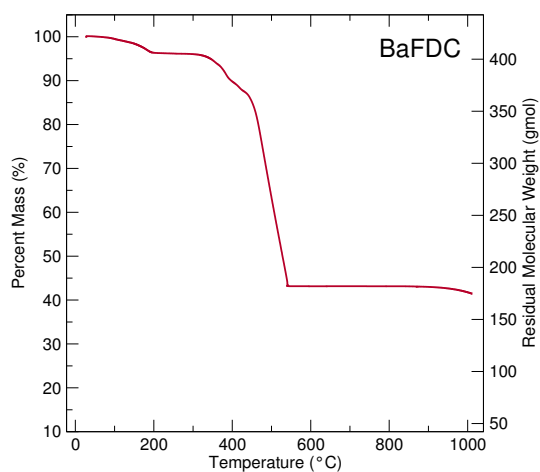
Figure 19 Thermogravimetric analysis of BaFDC in air.
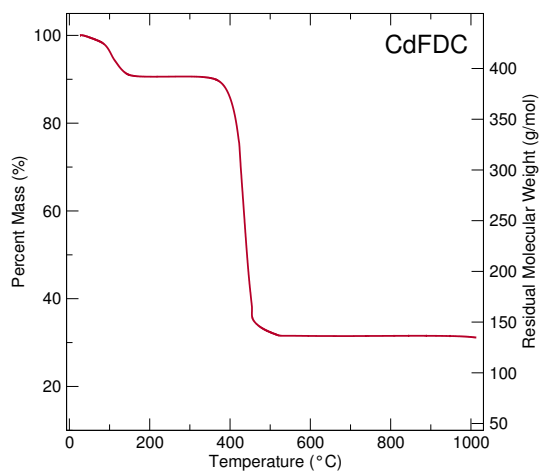
Figure 20 Thermogravimetric analysis of CdFDC in air.
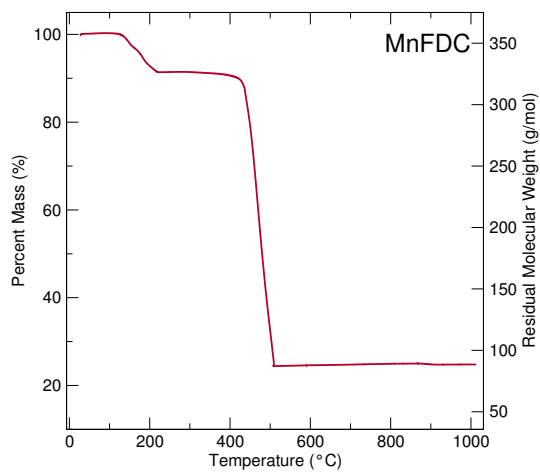
Figure 21 Thermogravimetric analysis of MnFDC in air.
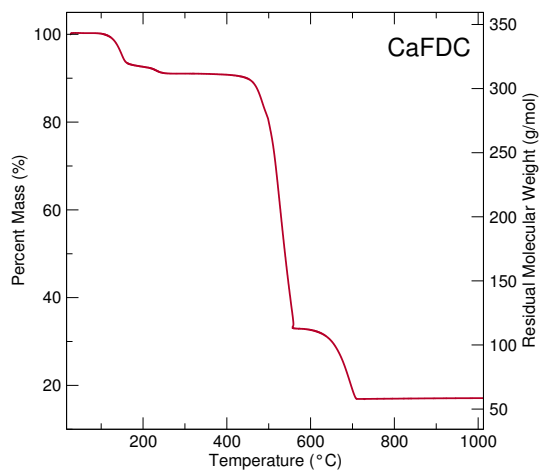
Figure 22 Thermogravimetric analysis of CaFDC in air.
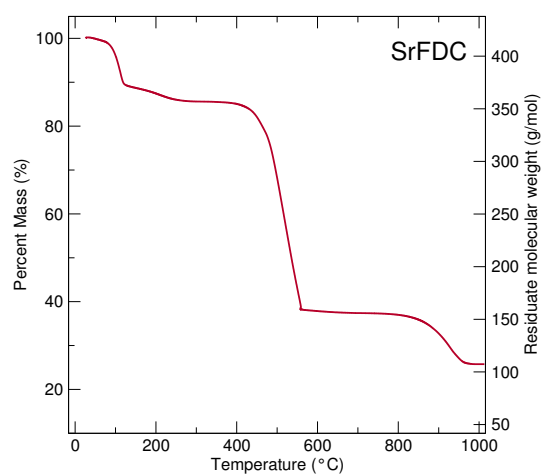
Figure 23 Thermogravimetric analysis of SrFDC in air.

4   Crystallographic details

4.1   Structure determination methods

All structures were determined using single crystal X-ray diffraction. Only very small crystals were available and so the high flux of the synchrotron radiation was needed. Data collection for was performed at beamline 11.3.1 on the Advanced Light Source at Lawrence Berkeley National Laboratory (λ=0.7749 Å). The beamline provides a flux of 1×10^{11} photons/s/0.01%BW at 10 keV, at a wavelength of 0.77490 Å, about five orders of magnitude brighter than a typical lab X-ray source. Crystals were mounted on a Kaptan loop using paratone-N oil and placed in a N_2 cryostream at 100 K. Data were collected using a Bruker D8 goniometer and APEX2 detector. Data integration and corrections for Lorentz and polarization effects were performed using Bruker SAINT version 7.56a [11]. SADABS was used to perform absorption corrections.[12] For samples BaFDC and MnFDC, a true single crystal could not be found and so data was collected on a twin. CELL_NOW was used to determine that the orientation matrices and the domains were related by a 180° rotation around the reciprocal axis (001) [13]. The integration was performed with both matrices. TWINABS was used to produce a merged reflection file, for structure solution and initial refinement, and a split reflection file for for final structure refinement. These computational software methods allowed for the correct crystallographic cell to be identified and the intensity from the twinned reflections to be correctly assigned. A summary of the structural details of all 5 fluorenone frameworks, including those from Furman et al. [14], are included in Table 4 for reference. The dimensionality of the structures is described in terms of both the inorganic connectivity, where metal–oxygen–metal bonds give rise to an extended structure, and organic connectivity, where bonding through the ligands gives rise to the extended structure, as described in Cheetham et al.[15]. This is also given as a shorthand I^xO^y where x is the inorganic dimensionality and y is the organic dimensionality, and $x + y$ is the overall dimensionality of the structure. The crystal structure of the parent ligand has not been reported in the literature and attempts to recrystallize X-ray quality samples were unfortunately unsuccessful.

Table 4 Crystallographic data for fluorenone structures from single crystal diffraction data. Dimensionality is given as inorganic connectivity and the metal-oxygen-metal connectivity, as desribed in Cheetham et al.[15]

	BaFDC	CdFDC	MnFDC	CaFDC	SrFDC
Formula	$BaC_{15}O_6H_8$	$CdC_{15}O_8H_{12}$	$MnC_{15}O_7H_{10}$	$CaC_{15}O_7H_{10}$	$Sr_2C_{30}O_{17}H_{26}$
MW (g/mol)	421.55	432.65	357.17	342.31	833.75
System	Triclinic	Monoclinic	Monoclinic	Monoclinic	Triclinic
Space Group	$P1$	$P2_1/c$	$C2/c$	$P2_1$	$P\bar{1}$
a (Å)	6.7676(6)	7.7123(2)	26.943(2)	7.5411(16)	8.578(2)
b (Å)	7.2311(7)	28.5057(8)	7.2476(6)	6.6118(14)	11.836(3)
c (Å)	14.1591(13)	6.6459(2)	6.9261(5)	27.999(6)	15.626(4)
α (°)	82.763(2)	90.00	90.00	90	72.437(4)
β (°)	84.102(2)	105.050(2)	97.703(2)	97.065(3)	78.722(5)
γ (°)	66.047(2)	90.00	90.00	90	85.437(4)
V (Å³)	627.17(10)	1410.95(7)	1340.27(18)	1385.4(5)	1483.1(7)
Z	2	4	4	4	2
ρ (g/cm³)	2.232	2.037	1.770	1.641	1.867
μ (mm⁻¹)	3.994	1.982	1.287	0.613	3.683
Measurement Temp (K)	100	100	100	100	298
Radiation Source	Synchrotron	Synchrotron	Synchrotron	Synchrotron	Mok_α
Radiation λ (Å)	0.7749	0.7749	0.7749	0.7749	0.7107
Scan Mode	Omega	Omega	Omega	Omega	Omega
Absorption Correction	SADABS	SADABS	SADABS	SADABS	SADABS
Solution Method	SHELX, $\lvert F\rvert^2$	SHELX, $\lvert F\rvert^2$	SHELX, $\lvert F\rvert^2$	SHELX, $\lvert F\rvert^2$	SHELX, $\lvert F\rvert^2$
2θ Range (°)	3.17-33.59	3.08-33.61	3.95-33.60	2.97-29.36	4.834-51.953
data/parameters/restraints	3737/398/3	4304/235/15	2016/116/0	5824/440/130	5902/487/21
R1/wR2 [I>2σ(I)]	2.67%/6.87%	2.57%/6.76%	2.58%/6.31%	8.19%/21.84%	5.71%/18.06%
R1/wR2 (all data)	2.61%/6.83%	2.88%/6.95%	3.12%/6.60%	8.56%/22.22%	10.13%/13.00%
Goodness of Fit	1.054	1.044	1.044	1.046	1.03
Bound Water	1	2	2	2	$2\frac{1}{2}$
Pore Water	0	1	0	0	1
Inorg. Dimen.	2-D	0-D	0-D	0-D	1-D
M-O-M Dimen.	1-D	2-D	3-D	3-D	2-D
dimensionality	I^2O^1	I^0O^2	I^0O^3	I^0O^3	I^1O^2
π-π dist.	3.30Å	3.33Å	3.39Å	3.41Å	3.38Å

4.2 Powder X-ray diffraction

Figures 24, 25, 26, 27, and 28, show Rietveld refinements of the structures determined by single crystal to the powder X-ray diffraction data. Data for CaFDC and MnFDC were collected at the Advanced Photon Source synchrotron X-ray beamline 11-BM at λ=0.5892 Å. Data for SrFDC, BaFDC, and CdFDC were collected on a Bruker D8 with CuKα. Unit cell parameters and refinement statistics are summarized in Table 5.
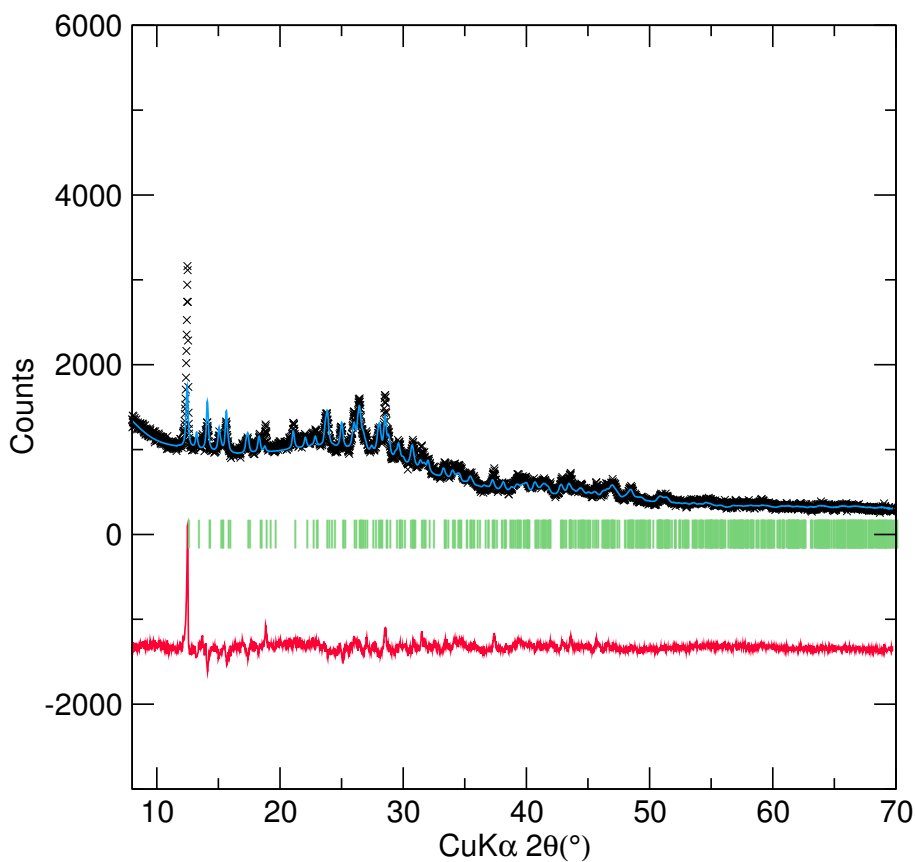
Figure 24 X-ray powder diffraction spectra of bulk sample of BaFDC and Rietveld refinement of model determined by single crystal diffraction (χ^2=5.592).

Table 5 Summary of refined Rietveld models to powder diffraction data

	BaFDC	CdFDC	MnFDC	CaFDC	SrFDC
Formula	$BaC_{15}O_6H_8$	$CdC_{15}O_8H_{12}$	$MnC_{15}O_7H_{10}$	$CaC_{15}O_7H_{10}$	$Sr_2C_{30}O_{17}H_{26}$
SG	$P1$	$P2_1/c$	$C2/c$	$P2_1$	$P\bar{1}$
a (Å)	6.7996(17)	7.7388(21)	26.89540(22)	7.5515(4)	8.5904(4)
b (Å)	7.2493(21)	28.502(6)	7.21464(6)	6.6325(3)	11.8583(6)
c (Å)	14.274(4)	6.7446(16)	6.99755(5)	27.962(1)	15.6506(7)
α (°)	82.836(33)	90.00	90.00	90	72.484(4)
β (°)	83.848(31)	105.286(23)	97.4052(11)	97.49(1)	78.663(4)
γ (°)	67.018(19)	90.00	90.00	90	85.464(4)
V (Å^3)	641.36(22)	1435.0(4)	1346.484(15)	1388.5(1)	1490.37(8)
χ^2	5.592	4.430	4.329	10.560	5.048
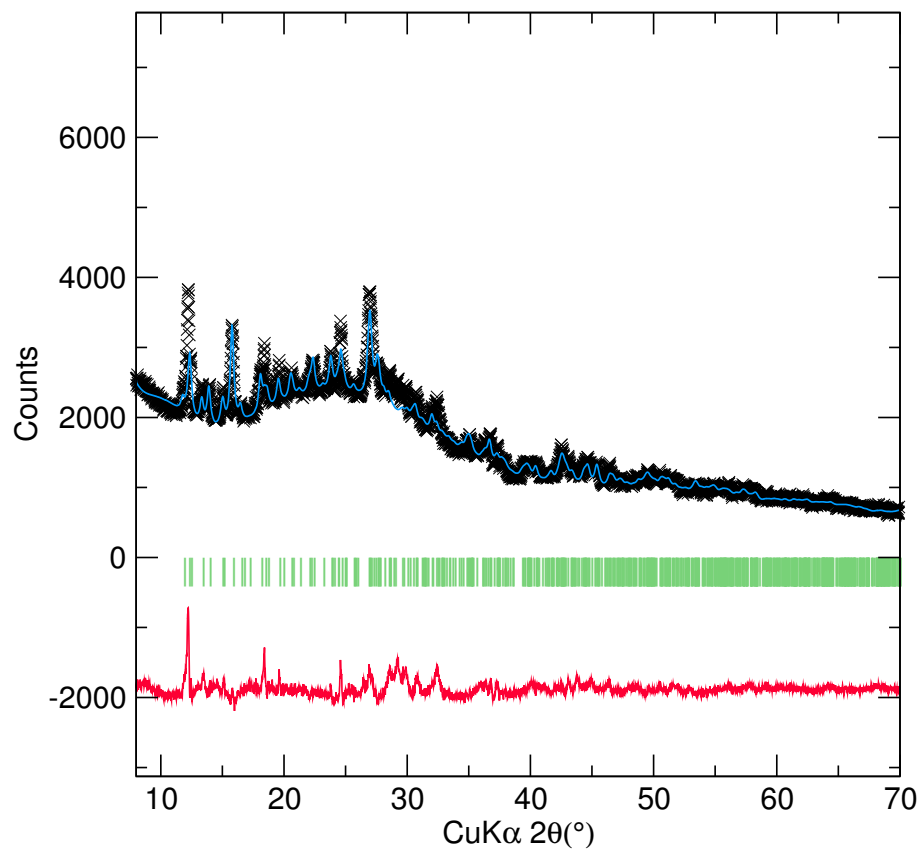
Figure 25 X-ray powder diffraction spectra of bulk sample of CdFDC and Rietveld refinement of model determined by single crystal diffraction (χ^2=4.430).
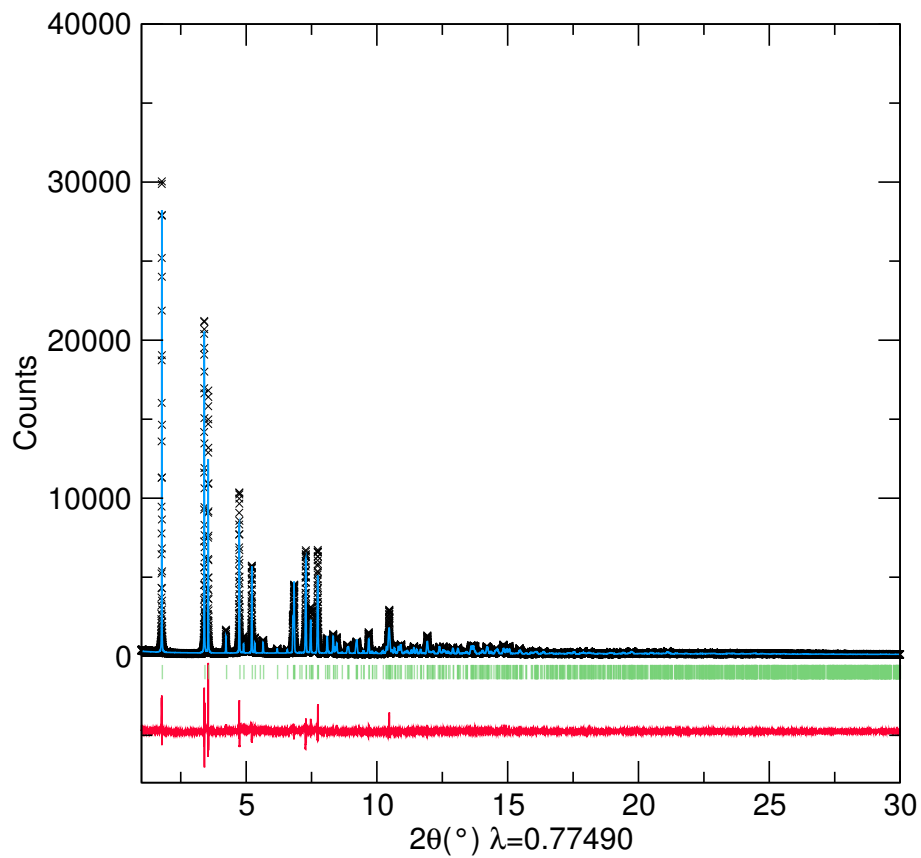
Figure 26 X-ray powder diffraction spectra of bulk sample of MnFDC and Rietveld refinement of model determined by single crystal diffraction (χ^2=4.329).
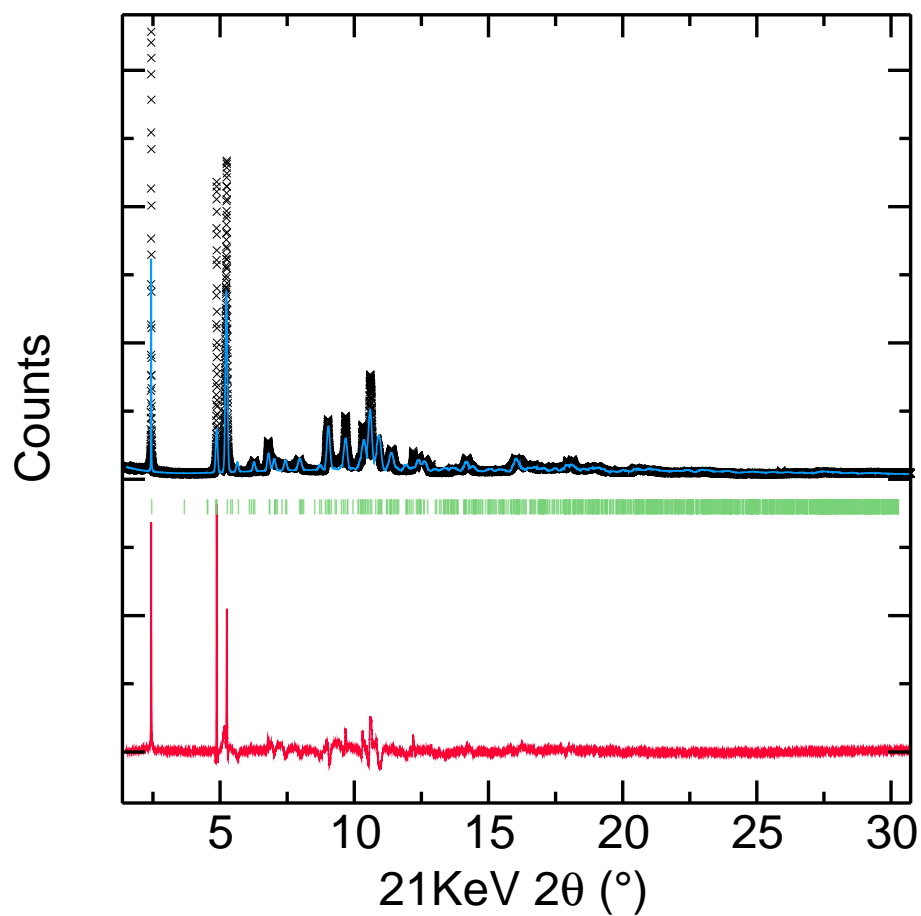
Figure 27 Synchrotron X-ray powder diffraction spectra (APS 11-BM, λ=0.7749 Å) of bulk sample of CaFDC and Rietveld refinement of model determined by single crystal diffraction (χ^2=10.560).
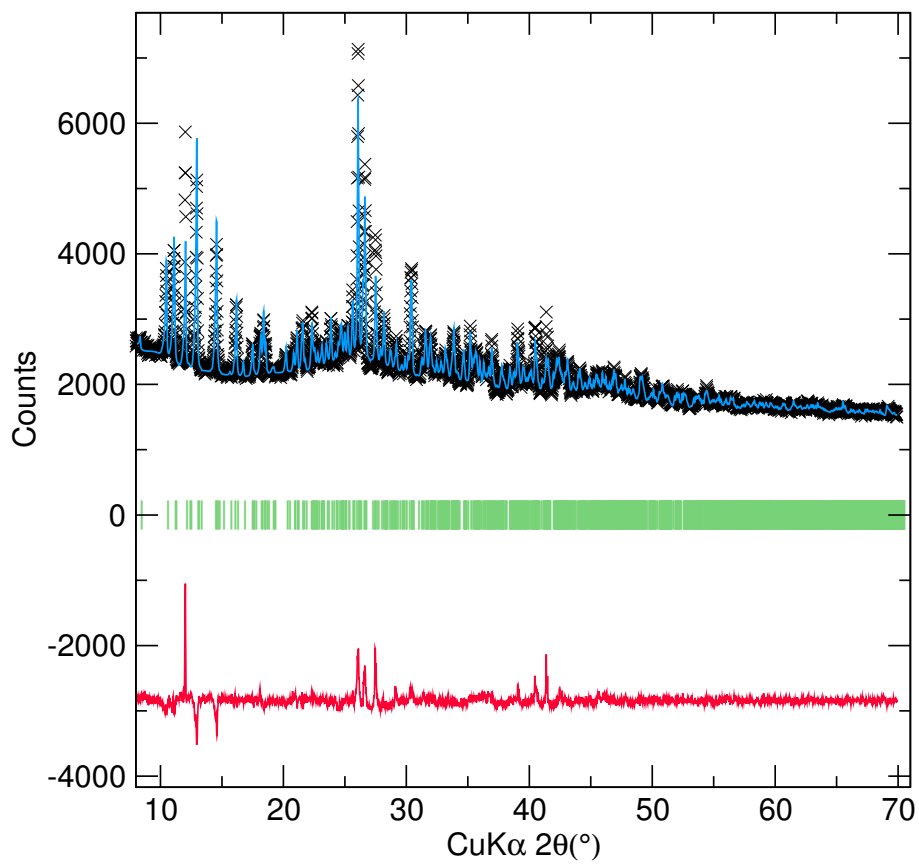
Figure 28 X-ray powder diffraction spectra of bulk sample of SrFDC and Rietveld refinement of model determined by single crystal diffraction (χ^2=5.046).

4.3   Additional crystal structure images

4.3.1   BaFDC
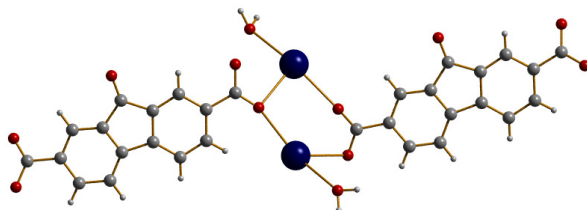
Figure 29 Asymmetric unit of BaFDC.
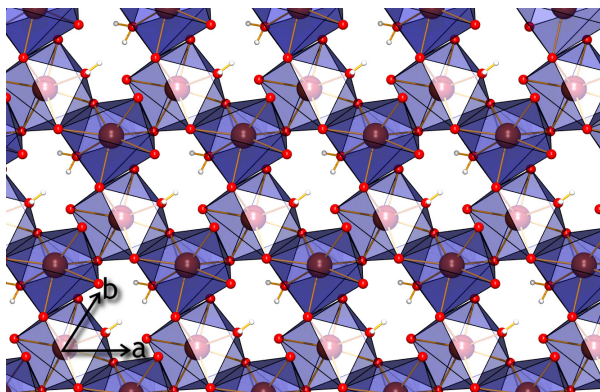
Figure 30 2-Dimensional inorganic sheet of BaFDC.

4.3.2   CdFDC
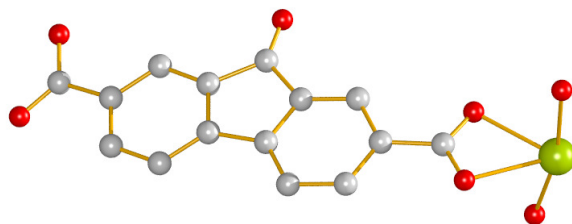
Figure 31 Asymmetric unit of CdFDC.
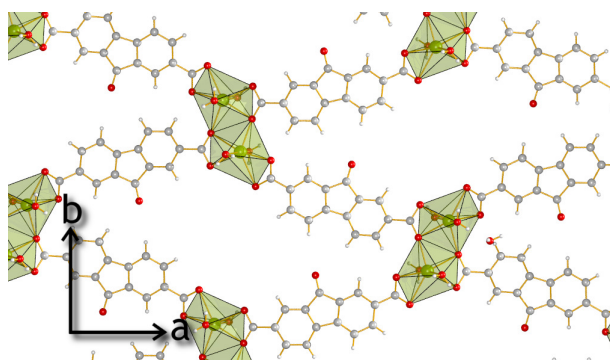
Figure 32 2-Dimensional inorganic sheet of CdFDC, pore waters omitted for clarity.

4.3.3   MnFDC
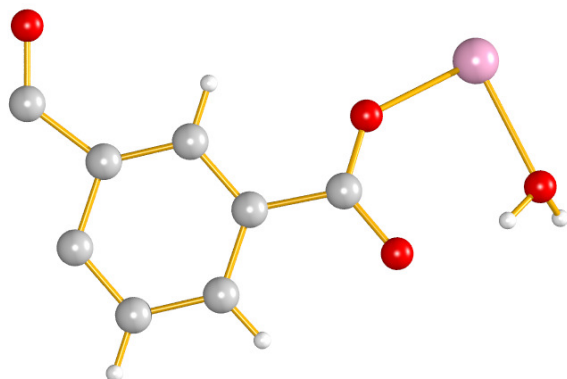
Figure 33 Asymmetric unit of MnFDC.

4.3.4 CaFDC

The structure of $Ca(FDC)(H_2O)_2$ **[4]**, shown in Figure 35, consists of isolated CaO_6 octahedra linked through FDC ligands. Each octahedron connects to four FDC ligand oxygen atoms and two coordinating water molecules, while each dicarboxylic acid oxygen atom of the FDC ligand is bound to a different metal. The octahedra arrange in sheets which are pillared by FDC ligands to form a 3-dimensional structure. The ligands are π-stacked with their ketone groups aligned at a separation of 3.41 Å.
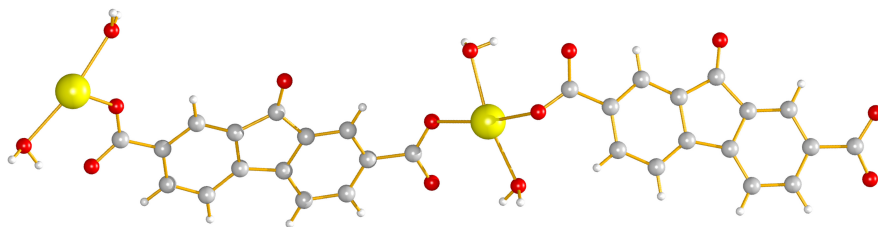
Figure 34 Asymmetric unit of CaFDC.
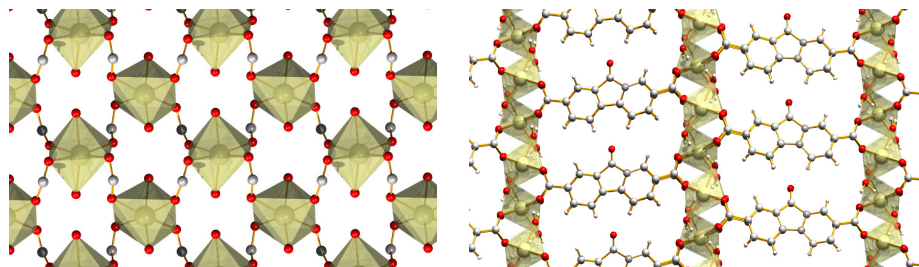
Figure 35 LEFT: Sheet of isolated CaO octahedra of CaFDC with hydrogen atoms omitted for clarity viewed down the c axis, RIGHT: The extended structure viewed down the a axis.

4.3.5 SrFDC

The structure of $Sr(FDC)(H_2O)_5 \cdot 2H_2O$ **[5]**, shown in Figure 36, consists of edge-sharing SrO_8 polyhedra that form 1-dimensional chains. These chains are linked in-plane by the carboxylic acid groups of the FDC ligand to form a sheet, and the sheets are in turn bridged by the FDC to form an extended 3-dimensional framework. The strontium atoms in the chains are arranged in pairs of two Sr1 atoms followed by two Sr2 atoms, with atom-atom distances of Sr1-Sr1 4.5674 Å, Sr1-Sr2 3.9935 Å, and Sr2-Sr2 4.0966 Å. The Sr1 polyhedra are completed by 2 coordinating water molecules, 3 bridging water molecules, and 3 oxygen atoms from ligand carboxylic acid groups. The Sr2 polyhedra consists of 1 coordinating water, 1 bridging water, and 6 oxygen atoms from the ligand. Two unbound water molecules sit in the pore space. One of the four oxygen atoms from the two dicarboxylic acid grounds on each FDC ligand is uncoordinated. The ligands π-stack less perfectly than those of CaFDC, with the ketone groups alternating in direction and a separation of 3.38 Å.
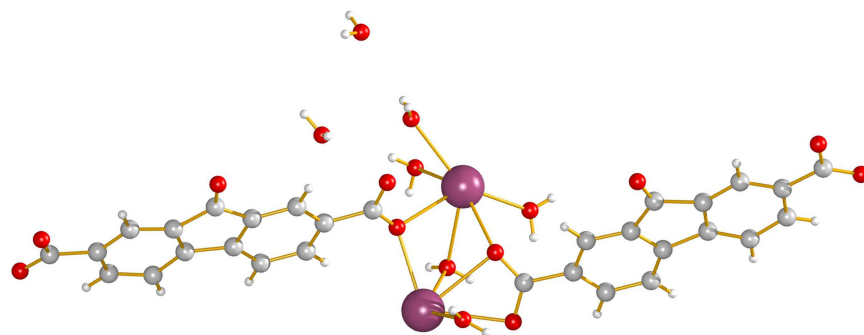
Figure 36 Asymmetric unit of SrFDC.
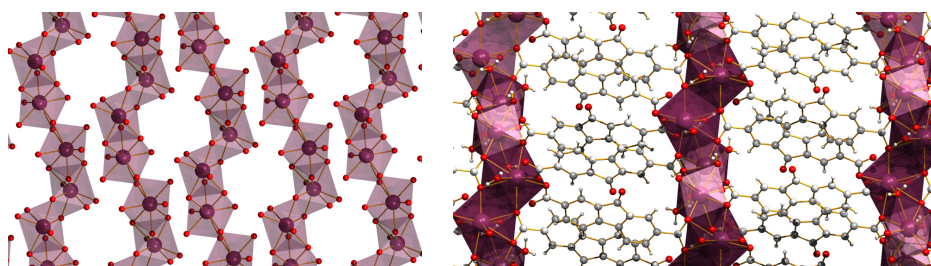
Figure 37 LEFT: 1-Dimensional edge sharing SrO_8 chains in SrFDC, hydrogen and carbon atoms omitted for clarity. RIGHT: Extended structure of SrFDC.

4.4 BaFDC structure details
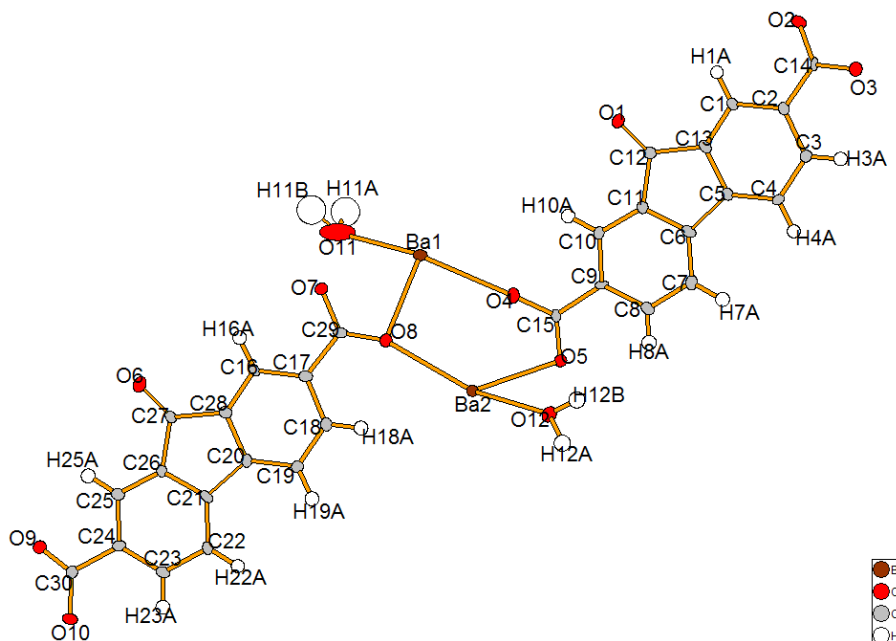
Figure 38 Asymmetric unit with atom numbers for BaFDC.

Table 6 Crystal data and structure refinement for BaFDC.

Parameter	Value
Empirical formula	$C_{15}H_8BaO_6$
Formula weight	$421.55\,\mathrm{g\cdot mol}^{-1}$
Collection Temperature	100(2) K
Wavelength	0.77490Å
Crystal system	Triclinic
Space Group	P1
Unit cell dimensions	
a	6.7676(6) Å
b	7.2311(7) Å
c	14.1591(13) Å
α	82.763(2)°
β	84.102(2)°
γ	66.047(2)°
Volume	627.17(10)Å^3
Z	2
Calculated density	2.232 g/m^3
Absorption coefficient	3.994 mm^{-1}
F(000)	404
Crystal size	0.12×0.08×0.02 mm
Theta range for data collection	3.17° to 33.59°
Limiting indices	$-9 \leq h \leq 9, -10 \leq k \leq 10, 0 \leq l \leq 20$
Reflections collected / unique	3737 / 3737 [R(int) = 0.0000]
Data Completeness	99.1%
Absorption correction	Semi-empirical from equivalents
Max. and min. transmission	0.9244 and 0.6457
Refinement method	Full-matrix least-squares on F^2
Data / restraints / parameters	3737 / 9 / 410
Goodness-of-fit on F^2	1.038
Final R indices [I>2sigma(I)]	R1 = 0.0258, wR2 = 0.0672
R indices (all data)	R1 = 0.0265, wR2 = 0.0676
Absolute Structure Parameter	0.143(19)
Largest diff. peak and hole	1.908 and -1.173 $e\cdot$Å^{-3}

Table 7 Crystal coordinates [Å] and equivalent isotropic displacement parameters [Å^2] for BaFDC. U$_{eq}$ is defined as one third of the trace of the orthogonalized U$_{ij}$ tensor.

	x	y	z	U$_{eq}$
Ba(1)	-0.44487(4)	0.07349(4)	0.48041(2)	0.01216(10)
Ba(2)	-0.10026(3)	0.43896(3)	0.39963(2)	0.01129(10)
O(1)	-0.5169(8)	0.1401(7)	0.9451(4)	0.0159(8)
O(2)	-0.6843(8)	0.3213(9)	1.3228(4)	0.0164(9)
O(3)	-0.5113(8)	0.5070(8)	1.3557(4)	0.0143(8)
O(4)	-0.3654(9)	0.3670(9)	0.5651(4)	0.0142(11)
O(5)	-0.3644(12)	0.6748(11)	0.5374(5)	0.0152(13)
O(6)	-0.0202(8)	-0.3636(7)	-0.0542(4)	0.0169(9)
O(7)	-0.1613(13)	-0.1851(11)	0.3246(5)	0.0183(14)
O(8)	-0.1378(10)	0.1079(9)	0.3438(4)	0.0144(11)
O(9)	-0.0554(7)	-0.0692(7)	-0.4314(4)	0.0126(8)
O(10)	0.1329(8)	0.1247(8)	-0.4699(4)	0.0139(8)
C(1)	-0.5581(9)	0.3632(9)	1.1263(4)	0.0104(10)
H(1A)	-0.5864	0.2454	1.1463	0.012
C(2)	-0.5518(12)	0.4882(12)	1.1929(6)	0.0112(13)
C(3)	-0.5089(10)	0.6625(9)	1.1615(5)	0.0118(10)
H(3A)	-0.4985	0.7428	1.2074	0.014
C(4)	-0.4810(9)	0.7204(9)	1.0634(4)	0.0109(10)
H(4A)	-0.4572	0.8402	1.0427	0.013
C(5)	-0.4899(11)	0.5947(10)	0.9985(5)	0.0115(11)
C(6)	-0.4653(10)	0.6111(10)	0.8928(5)	0.0118(10)
C(7)	-0.4283(10)	0.7556(9)	0.8283(4)	0.0123(10)
H(7A)	-0.4183	0.8711	0.8491	0.015
C(8)	-0.4062(10)	0.7262(10)	0.7319(4)	0.0132(11)
H(8A)	-0.3778	0.8228	0.6869	0.016
C(9)	-0.4242(11)	0.5602(9)	0.6985(4)	0.0105(10)
C(10)	-0.4623(10)	0.4142(9)	0.7643(4)	0.0120(10)
H(10A)	-0.4739	0.2993	0.7436	0.014
C(11)	-0.4825(11)	0.4424(9)	0.8603(5)	0.0108(10)
C(12)	-0.5115(10)	0.3060(9)	0.9450(4)	0.0115(10)
C(13)	-0.5223(10)	0.4155(9)	1.0309(5)	0.0110(10)
C(14)	-0.5848(13)	0.4368(12)	1.2959(6)	0.0079(15)
C(15)	-0.3867(16)	0.5346(15)	0.5940(7)	0.0115(17)
C(16)	-0.0592(10)	-0.1337(9)	0.1242(4)	0.0113(10)
H(16A)	-0.0886	-0.2502	0.1461	0.014
C(17)	-0.0563(11)	-0.0013(10)	0.1884(5)	0.0123(11)
C(18)	-0.0085(10)	0.1685(9)	0.1542(4)	0.0127(10)
H(18A)	-0.0034	0.2545	0.1985	0.015
C(19)	0.0313(10)	0.2140(9)	0.0575(4)	0.0125(10)
H(19A)	0.0643	0.3286	0.0359	0.015
C(20)	0.0217(10)	0.0876(9)	-0.0066(5)	0.0107(10)
C(21)	0.0442(11)	0.0977(9)	-0.1123(5)	0.0116(10)
C(22)	0.0797(9)	0.2399(9)	-0.1800(4)	0.0109(10)
H(22A)	0.0975	0.3535	-0.1613	0.013
C(23)	0.0884(10)	0.2104(9)	-0.2767(4)	0.0126(10)
H(23A)	0.1181	0.3029	-0.3238	0.015
C(24)	0.0543(13)	0.0485(12)	-0.3049(6)	0.0110(14)
C(25)	0.0199(10)	-0.0948(10)	-0.2369(4)	0.0122(10)
H(25A)	-0.0021	-0.2066	-0.2554	0.015
C(26)	0.0187(12)	-0.0685(9)	-0.1420(5)	0.0110(11)
C(27)	-0.0113(10)	-0.1995(10)	-0.0556(4)	0.0121(10)
C(28)	-0.0177(10)	-0.0883(9)	0.0278(5)	0.0101(10)
C(29)	-0.1224(17)	-0.0266(16)	0.2925(7)	0.0126(18)
C(30)	0.0461(17)	0.0287(13)	-0.4104(7)	0.0144(18)
O(11)	-0.6402(14)	-0.0838(15)	0.3743(8)	0.052(3)
H(11A)	-0.777(10)	-0.06(2)	0.399(10)	0.063
H(11B)	-0.65(2)	-0.205(11)	0.368(11)	0.063
O(12)	0.1560(10)	0.5540(10)	0.5035(5)	0.0167(12)
H(12A)	0.228(14)	0.635(12)	0.489(6)	0.020
H(12B)	0.172(16)	0.563(15)	0.565(2)	0.020

Table 8 Anisotropic displacement parameters [Å^2] for BaFDC. The anisotropic displacement factor exponent takes the form $-2\pi^2[h^2a^{*2}U^{11} + ... + 2hka^*b^*U^{12}]$.

	U^{11}	U^{22}	U^{33}	U^{23}	U^{13}	U^{12}
Ba(1)	0.0116(2)	0.0126(2)	0.0121(2)	0.00142(17)	-0.00002(17)	-0.00554(18)
Ba(2)	0.0129(2)	0.0134(2)	0.0099(2)	-0.00139(16)	0.00025(16)	-0.00773(18)
O(1)	0.020(2)	0.011(2)	0.016(2)	-0.0034(16)	0.0010(17)	-0.0065(17)
O(2)	0.018(2)	0.026(3)	0.011(2)	-0.0007(19)	0.0007(17)	-0.015(2)
O(3)	0.015(2)	0.016(2)	0.014(2)	-0.0027(17)	-0.0017(16)	-0.0077(18)
O(4)	0.016(2)	0.013(3)	0.013(2)	-0.0034(19)	-0.0023(18)	-0.004(2)
O(5)	0.021(2)	0.012(2)	0.014(3)	-0.003(2)	0.004(2)	-0.008(2)
O(6)	0.020(2)	0.012(2)	0.019(2)	-0.0036(17)	-0.0012(17)	-0.0057(17)
O(7)	0.031(3)	0.018(3)	0.012(3)	-0.001(2)	0.000(2)	-0.017(3)
O(8)	0.016(2)	0.014(3)	0.015(3)	-0.005(2)	0.004(2)	-0.008(2)
O(9)	0.0139(19)	0.0095(19)	0.013(2)	0.0003(16)	-0.0021(16)	-0.0032(16)
O(10)	0.0143(19)	0.019(2)	0.011(2)	0.0025(18)	-0.0017(17)	-0.0105(18)
C(1)	0.010(2)	0.013(3)	0.009(2)	-0.0024(19)	0.0013(19)	-0.005(2)
C(2)	0.010(3)	0.013(3)	0.010(3)	-0.003(2)	0.001(2)	-0.005(2)
C(3)	0.012(2)	0.013(3)	0.013(3)	-0.003(2)	0.002(2)	-0.007(2)
C(4)	0.012(2)	0.009(2)	0.013(3)	-0.0012(19)	0.0013(19)	-0.006(2)
C(5)	0.011(3)	0.014(3)	0.010(3)	-0.003(2)	0.001(2)	-0.006(2)
C(6)	0.007(2)	0.019(3)	0.010(3)	0.000(2)	0.000(2)	-0.007(2)
C(7)	0.012(2)	0.011(2)	0.012(2)	-0.0018(19)	-0.005(2)	-0.002(2)
C(8)	0.015(2)	0.014(3)	0.010(2)	0.000(2)	0.000(2)	-0.005(2)
C(9)	0.012(3)	0.006(2)	0.011(3)	0.0043(19)	-0.001(2)	-0.003(2)
C(10)	0.014(2)	0.011(2)	0.012(2)	-0.004(2)	0.001(2)	-0.006(2)
C(11)	0.011(2)	0.010(3)	0.011(3)	-0.0025(19)	0.000(2)	-0.003(2)
C(12)	0.012(2)	0.013(2)	0.011(2)	0.000(2)	-0.0011(19)	-0.006(2)
C(13)	0.011(2)	0.014(3)	0.008(2)	-0.0007(19)	-0.001(2)	-0.004(2)
C(14)	0.007(3)	0.008(3)	0.009(3)	-0.004(2)	-0.003(2)	-0.002(2)
C(15)	0.014(3)	0.013(4)	0.010(3)	-0.005(3)	0.002(3)	-0.007(3)
C(16)	0.014(2)	0.014(3)	0.006(2)	-0.0014(19)	0.0001(19)	-0.006(2)
C(17)	0.011(3)	0.011(3)	0.013(3)	0.000(2)	0.002(2)	-0.004(2)
C(18)	0.015(2)	0.011(3)	0.012(3)	-0.003(2)	0.001(2)	-0.004(2)
C(19)	0.016(3)	0.013(3)	0.011(2)	-0.0011(19)	-0.001(2)	-0.008(2)
C(20)	0.008(2)	0.012(3)	0.013(3)	-0.006(2)	0.003(2)	-0.004(2)
C(21)	0.012(2)	0.015(3)	0.008(3)	-0.002(2)	0.003(2)	-0.005(2)
C(22)	0.011(2)	0.011(2)	0.010(2)	-0.0034(19)	0.0002(19)	-0.003(2)
C(23)	0.012(2)	0.013(3)	0.011(3)	0.001(2)	0.001(2)	-0.005(2)
C(24)	0.012(3)	0.011(3)	0.012(3)	0.001(2)	-0.001(2)	-0.006(2)
C(25)	0.013(2)	0.015(3)	0.011(3)	0.000(2)	-0.001(2)	-0.008(2)
C(26)	0.015(3)	0.010(3)	0.008(3)	-0.001(2)	-0.002(2)	-0.005(2)
C(27)	0.015(2)	0.017(3)	0.008(2)	-0.003(2)	0.0010(19)	-0.009(2)
C(28)	0.007(2)	0.010(3)	0.011(3)	-0.0004(19)	0.000(2)	-0.0014(19)
C(29)	0.015(4)	0.013(4)	0.010(3)	0.003(3)	-0.003(2)	-0.006(3)
C(30)	0.019(3)	0.009(4)	0.014(3)	-0.003(3)	0.003(3)	-0.005(3)
O(11)	0.026(4)	0.037(5)	0.072(7)	0.021(4)	0.017(4)	-0.003(3)
O(12)	0.012(3)	0.022(3)	0.021(3)	-0.005(2)	-0.001(2)	-0.012(2)

Table 9 Symmetry operations used in the following tables for BaFDC.

	Operation
#1	'x,y,z'

Table 10 Bond Lengths [Å] for BaFDC.

	Angle	Symm. op. atom 1	Symm. op. atom 3
Ba(1)-O(5)	2.737(7)	1	
Ba(1)-O(10)	2.755(5)	1	
Ba(1)-O(8)	2.756(6)		
Ba(1)-O(9)	2.778(5)	1	
Ba(1)-O(4)	2.817(6)		
Ba(1)-O(2)	2.863(5)	1	
Ba(1)-O(7)	3.050(7)		
Ba(1)-C(29)	3.221(11)		
Ba(1)-O(3)	3.282(5)	1	
Ba(1)-C(14)	3.374(9)	1	
Ba(1)-Ba(2)	4.1745(4)		
Ba(2)-O(7)	2.672(7)	1	
Ba(2)-O(8)	2.726(6)		
Ba(2)-O(2)	2.737(5)	1	
Ba(2)-O(3)	2.745(5)	1	
Ba(2)-O(5)	2.749(7)		
Ba(2)-O(10)	2.774(5)	1	
Ba(2)-O(12)	2.805(6)		
Ba(2)-O(4)	2.927(6)		
Ba(2)-C(15)	3.178(10)		
Ba(2)-Ba(1)	4.3277(5)	1	
Ba(2)-Ba(1)	4.4593(5)	1	
O(1)-C(12)	1.215(8)		
O(2)-C(14)	1.273(10)		
O(2)-Ba(2)	2.737(5)	1	
O(2)-Ba(1)	2.863(5)	1	
O(3)-C(14)	1.274(9)		
O(3)-Ba(2)	2.745(5)	1	
O(3)-Ba(1)	3.282(5)	1	
O(4)-C(15)	1.275(11)		
O(5)-C(15)	1.259(12)		
O(5)-Ba(1)	2.737(7)	1	
O(6)-C(27)	1.210(8)		
O(7)-C(29)	1.296(12)		
O(7)-Ba(2)	2.672(7)	1	
O(8)-C(29)	1.251(12)		
O(9)-C(30)	1.245(11)		
O(9)-Ba(1)	2.778(5)	1	
O(10)-C(30)	1.272(11)		
O(10)-Ba(1)	2.755(5)	1	
O(10)-Ba(2)	2.774(5)	1	
C(1)-C(13)	1.381(8)		
C(1)-C(2)	1.401(10)		
C(1)-H(1A)	0.9500		
C(2)-C(3)	1.414(10)		
C(2)-C(14)	1.476(12)		
C(3)-C(4)	1.415(8)		
C(3)-H(3A)	0.9500		
C(4)-C(5)	1.393(8)		
C(4)-H(4A)	0.9500		
C(5)-C(13)	1.413(9)		
C(5)-C(6)	1.484(9)		
C(6)-C(7)	1.383(8)		
C(6)-C(11)	1.408(9)		
C(7)-C(8)	1.391(8)		
C(7)-H(7A)	0.9500		
C(8)-C(9)	1.397(9)		
C(8)-H(8A)	0.9500		
C(9)-C(10)	1.405(9)		
C(9)-C(15)	1.498(12)		

Table 11 Continued: Bond Lengths [Å] for BaFDC.

	Angle	Symm. op. atom 1	Symm. op. atom 3
C(10)-C(11)	1.383(8)		
C(10)-H(10A)	0.9500		
C(11)-C(12)	1.504(9)		
C(12)-C(13)	1.513(9)		
C(14)-Ba(1)	3.374(9)	1	
C(16)-C(28)	1.391(8)		
C(16)-C(17)	1.407(9)		
C(16)-H(16A)	0.9500		
C(17)-C(18)	1.409(9)		
C(17)-C(29)	1.507(12)		
C(18)-C(19)	1.392(8)		
C(18)-H(18A)	0.9500		
C(19)-C(20)	1.392(8)		
C(19)-H(19A)	0.9500		
C(20)-C(28)	1.421(9)		
C(20)-C(21)	1.483(9)		
C(21)-C(22)	1.393(8)		
C(21)-C(26)	1.400(9)		
C(22)-C(23)	1.403(8)		
C(22)-H(22A)	0.9500		
C(23)-C(24)	1.393(10)		
C(23)-H(23A)	0.9500		
C(24)-C(25)	1.398(10)		
C(24)-C(30)	1.527(13)		
C(25)-C(26)	1.379(9)		
C(25)-H(25A)	0.9500		
C(26)-C(27)	1.499(10)		
C(27)-C(28)	1.498(9)		
O(11)-H(11A)	0.90(2)		
O(11)-H(11B)	0.91(2)		
O(12)-H(12A)	0.89(2)		
O(12)-H(12B)	0.90(2)		

Table 12 Bond Angles [°] for BaFDC.

	Angle	Symm. op. atom 1	Symm. op. atom 3
O(5)-Ba(1)-O(8)	111.2(2)	1	
O(10)-Ba(1)-O(8)	149.37(16)	1	
O(11)-Ba(1)-O(9)	135.9(2)		1
O(5)-Ba(1)-O(9)	76.03(19)	1	1
O(10)-Ba(1)-O(9)	137.60(14)	1	1
O(8)-Ba(1)-O(9)	73.03(16)		1
O(11)-Ba(1)-O(4)	159.0(2)		
O(5)-Ba(1)-O(4)	131.69(19)	1	
O(10)-Ba(1)-O(4)	107.69(17)	1	
O(8)-Ba(1)-O(4)	83.77(18)		
O(9)-Ba(1)-O(4)	64.70(15)	1	
O(11)-Ba(1)-O(2)	60.9(2)		1
O(5)-Ba(1)-O(2)	128.0(2)	1	1
O(10)-Ba(1)-O(2)	75.35(14)	1	1
O(8)-Ba(1)-O(2)	74.70(16)		1
O(9)-Ba(1)-O(2)	145.48(14)	1	1
O(4)-Ba(1)-O(2)	100.00(16)		1
O(11)-Ba(1)-O(7)	63.5(2)		
O(5)-Ba(1)-O(7)	71.55(18)	1	
O(10)-Ba(1)-O(7)	124.44(19)	1	
O(8)-Ba(1)-O(7)	45.03(19)		
O(9)-Ba(1)-O(7)	82.76(18)	1	
O(4)-Ba(1)-O(7)	126.38(19)		
O(2)-Ba(1)-O(7)	83.13(19)	1	
O(11)-Ba(1)-C(29)	77.7(3)		
O(5)-Ba(1)-C(29)	94.3(2)	1	
O(10)-Ba(1)-C(29)	136.7(2)	1	
O(8)-Ba(1)-C(29)	22.5(2)		
O(9)-Ba(1)-C(29)	81.8(2)	1	
O(4)-Ba(1)-C(29)	106.2(2)		
O(2)-Ba(1)-C(29)	72.9(2)	1	
O(7)-Ba(1)-C(29)	23.6(2)		
O(11)-Ba(1)-O(3)	101.8(2)		1
O(5)-Ba(1)-O(3)	164.73(16)	1	1
O(10)-Ba(1)-O(3)	101.62(13)	1	1
O(8)-Ba(1)-O(3)	58.28(16)		1
O(9)-Ba(1)-O(3)	108.51(13)	1	1
O(4)-Ba(1)-O(3)	61.30(14)		1
O(2)-Ba(1)-O(3)	41.71(13)	1	1
O(7)-Ba(1)-O(3)	94.27(16)		1
C(29)-Ba(1)-O(3)	72.4(2)		1
O(11)-Ba(1)-C(14)	80.0(2)		1
O(5)-Ba(1)-C(14)	144.5(2)	1	1
O(10)-Ba(1)-C(14)	93.32(17)	1	1
O(8)-Ba(1)-C(14)	59.2(2)		1
O(9)-Ba(1)-C(14)	124.72(18)	1	1
O(4)-Ba(1)-C(14)	83.18(18)		1
O(2)-Ba(1)-C(14)	21.62(16)	1	1
O(7)-Ba(1)-C(14)	82.3(2)		1
C(29)-Ba(1)-C(14)	64.8(2)		1
O(3)-Ba(1)-C(14)	22.01(15)	1	1
O(11)-Ba(1)-Ba(2)	130.8(2)		
O(5)-Ba(1)-Ba(2)	138.87(16)	1	
O(10)-Ba(1)-Ba(2)	137.80(11)	1	
O(8)-Ba(1)-Ba(2)	40.14(12)		
O(9)-Ba(1)-Ba(2)	67.71(10)	1	
O(4)-Ba(1)-Ba(2)	44.43(12)		
O(2)-Ba(1)-Ba(2)	79.78(10)	1	
O(7)-Ba(1)-Ba(2)	84.92(14)		
C(29)-Ba(1)-Ba(2)	62.54(18)		

Table 13 Continued: Bond Angles [°] for BaFDC.

	Angle	Symm. op. atom 1	Symm. op. atom 3
O(3)-Ba(1)-Ba(2)	41.05(8)	1	
C(14)-Ba(1)-Ba(2)	58.16(14)	1	
O(7)-Ba(2)-O(8)	137.0(2)	1	
O(7)-Ba(2)-O(2)	86.8(2)	1	1
O(8)-Ba(2)-O(2)	91.94(17)		1
O(7)-Ba(2)-O(3)	89.6(2)	1	1
O(8)-Ba(2)-O(3)	65.91(17)		1
O(2)-Ba(2)-O(3)	141.97(15)	1	1
O(7)-Ba(2)-O(5)	77.5(2)	1	
O(8)-Ba(2)-O(5)	124.76(19)		
O(2)-Ba(2)-O(5)	139.5(2)	1	
O(3)-Ba(2)-O(5)	75.75(19)	1	
O(7)-Ba(2)-O(10)	143.8(2)	1	1
O(8)-Ba(2)-O(10)	76.44(17)		1
O(2)-Ba(2)-O(10)	77.10(15)	1	1
O(3)-Ba(2)-O(10)	122.68(15)	1	1
O(5)-Ba(2)-O(10)	94.02(19)		1
O(7)-Ba(2)-O(12)	75.3(2)	1	
O(8)-Ba(2)-O(12)	142.56(19)		
O(2)-Ba(2)-O(12)	67.94(18)	1	
O(3)-Ba(2)-O(12)	146.61(16)	1	
O(5)-Ba(2)-O(12)	72.0(2)		
O(10)-Ba(2)-O(12)	68.62(18)	1	
O(7)-Ba(2)-O(4)	121.51(19)	1	
O(8)-Ba(2)-O(4)	82.24(16)		
O(2)-Ba(2)-O(4)	143.43(16)	1	
O(3)-Ba(2)-O(4)	67.02(16)	1	
O(5)-Ba(2)-O(4)	45.8(2)		
O(10)-Ba(2)-O(4)	66.41(15)	1	
O(12)-Ba(2)-O(4)	95.41(17)		
O(7)-Ba(2)-C(15)	100.5(2)	1	
O(8)-Ba(2)-C(15)	105.6(2)		
O(2)-Ba(2)-C(15)	143.1(2)	1	
O(3)-Ba(2)-C(15)	74.7(2)	1	
O(5)-Ba(2)-C(15)	23.1(2)		
O(10)-Ba(2)-C(15)	76.0(2)	1	
O(12)-Ba(2)-C(15)	79.0(2)		
O(4)-Ba(2)-C(15)	23.7(2)		
O(7)-Ba(2)-Ba(1)	140.57(17)	1	
O(8)-Ba(2)-Ba(1)	40.67(12)		
O(2)-Ba(2)-Ba(1)	127.43(12)	1	
O(3)-Ba(2)-Ba(1)	51.75(11)	1	
O(5)-Ba(2)-Ba(1)	84.42(15)		
O(10)-Ba(2)-Ba(1)	71.38(10)	1	
O(12)-Ba(2)-Ba(1)	131.29(13)		
O(4)-Ba(2)-Ba(1)	42.35(12)		
C(15)-Ba(2)-Ba(1)	65.21(17)		
O(7)-Ba(2)-Ba(1)	113.87(17)	1	1
O(8)-Ba(2)-Ba(1)	91.04(13)		1
O(2)-Ba(2)-Ba(1)	40.46(11)	1	1
O(3)-Ba(2)-Ba(1)	155.53(11)	1	1
O(5)-Ba(2)-Ba(1)	114.53(16)		1
O(10)-Ba(2)-Ba(1)	38.34(10)	1	1
O(12)-Ba(2)-Ba(1)	52.93(13)		1
O(4)-Ba(2)-Ba(1)	103.30(11)		1
C(15)-Ba(2)-Ba(1)	105.79(19)		1
Ba(1)-Ba(2)-Ba(1)	105.483(11)		1
O(7)-Ba(2)-Ba(1)	41.96(15)	1	1
O(8)-Ba(2)-Ba(1)	146.56(13)		1
O(2)-Ba(2)-Ba(1)	118.51(12)	1	1

Table 14 Continued: Bond Angles [°] for BaFDC.

	Angle	Symm. op. atom 1	Symm. op. atom 3
O(3)-Ba(2)-Ba(1)	80.98(10)	1	1
O(5)-Ba(2)-Ba(1)	35.53(15)		1
O(10)-Ba(2)-Ba(1)	121.26(12)	1	1
O(12)-Ba(2)-Ba(1)	67.83(13)		1
O(4)-Ba(2)-Ba(1)	80.59(12)		1
C(15)-Ba(2)-Ba(1)	58.63(18)		1
Ba(1)-Ba(2)-Ba(1)	113.720(10)		1
Ba(1)-Ba(2)-Ba(1)	120.758(9)	1	1
C(14)-O(2)-Ba(2)	126.3(5)		1
C(14)-O(2)-Ba(1)	102.4(5)		1
Ba(2)-O(2)-Ba(1)	101.19(16)	1	1
C(14)-O(3)-Ba(2)	133.3(5)		1
C(14)-O(3)-Ba(1)	83.1(5)		1
Ba(2)-O(3)-Ba(1)	87.20(13)	1	1
C(15)-O(4)-Ba(1)	162.3(6)		
C(15)-O(4)-Ba(2)	89.3(5)		
Ba(1)-O(4)-Ba(2)	93.22(17)		
C(15)-O(5)-Ba(1)	153.3(6)		1
C(15)-O(5)-Ba(2)	98.0(6)		
Ba(1)-O(5)-Ba(2)	108.8(2)	1	
C(29)-O(7)-Ba(2)	160.8(7)		1
C(29)-O(7)-Ba(1)	85.6(6)		
Ba(2)-O(7)-Ba(1)	102.2(2)	1	
C(29)-O(8)-Ba(2)	159.9(6)		
C(29)-O(8)-Ba(1)	100.1(6)		
Ba(2)-O(8)-Ba(1)	99.20(18)		
C(30)-O(9)-Ba(1)	128.7(5)		1
C(30)-O(10)-Ba(1)	133.7(6)		1
C(30)-O(10)-Ba(2)	123.1(6)		1
Ba(1)-O(10)-Ba(2)	103.01(15)	1	1
C(13)-C(1)-C(2)	118.3(6)		
C(13)-C(1)-H(1A)	120.9		
C(2)-C(1)-H(1A)	120.9		
C(1)-C(2)-C(3)	119.8(7)		
C(1)-C(2)-C(14)	120.4(7)		
C(3)-C(2)-C(14)	119.7(7)		
C(2)-C(3)-C(4)	121.7(6)		
C(2)-C(3)-H(3A)	119.1		
C(4)-C(3)-H(3A)	119.1		
C(5)-C(4)-C(3)	117.4(6)		
C(5)-C(4)-H(4A)	121.3		
C(3)-C(4)-H(4A)	121.3		
C(4)-C(5)-C(13)	120.4(6)		
C(4)-C(5)-C(6)	130.6(6)		
C(13)-C(5)-C(6)	109.0(5)		
C(7)-C(6)-C(11)	120.1(6)		
C(7)-C(6)-C(5)	131.2(6)		
C(11)-C(6)-C(5)	108.7(6)		
C(6)-C(7)-C(8)	117.9(6)		
C(6)-C(7)-H(7A)	121.1		
C(8)-C(7)-H(7A)	121.1		
C(7)-C(8)-C(9)	122.6(6)		
C(7)-C(8)-H(8A)	118.7		
C(9)-C(8)-H(8A)	118.7		
C(8)-C(9)-C(10)	119.2(6)		
C(8)-C(9)-C(15)	119.1(6)		
C(10)-C(9)-C(15)	121.5(7)		
C(11)-C(10)-C(9)	118.2(6)		
C(11)-C(10)-H(10A)	120.9		
C(9)-C(10)-H(10A)	120.9		

Table 15 Continued: Bond Angles [°] for BaFDC.

	Angle	Symm. op. atom 1	Symm. op. atom 3
C(10)-C(11)-C(6)	121.9(6)		
C(10)-C(11)-C(12)	129.1(6)		
C(6)-C(11)-C(12)	108.9(5)		
O(1)-C(12)-C(11)	127.7(6)		
O(1)-C(12)-C(13)	127.1(6)		
C(11)-C(12)-C(13)	105.1(5)		
C(1)-C(13)-C(5)	122.3(6)		
C(1)-C(13)-C(12)	129.6(6)		
C(5)-C(13)-C(12)	108.2(5)		
O(2)-C(14)-O(3)	121.6(8)		
O(2)-C(14)-C(2)	119.1(7)		
O(3)-C(14)-C(2)	119.4(7)		
O(2)-C(14)-Ba(1)	56.0(4)		1
O(3)-C(14)-Ba(1)	74.9(5)		1
C(2)-C(14)-Ba(1)	146.4(5)		1
O(5)-C(15)-O(4)	121.7(9)		
O(5)-C(15)-C(9)	119.0(8)		
O(4)-C(15)-C(9)	119.2(8)		
O(5)-C(15)-Ba(2)	58.9(5)		
O(4)-C(15)-Ba(2)	67.1(5)		
C(9)-C(15)-Ba(2)	154.7(6)		
C(28)-C(16)-C(17)	117.8(6)		
C(28)-C(16)-H(16A)	121.1		
C(17)-C(16)-H(16A)	121.1		
C(16)-C(17)-C(18)	119.9(6)		
C(16)-C(17)-C(29)	121.2(7)		
C(18)-C(17)-C(29)	118.7(7)		
C(19)-C(18)-C(17)	122.1(6)		
C(19)-C(18)-H(18A)	119.0		
C(17)-C(18)-H(18A)	119.0		
C(18)-C(19)-C(20)	118.4(6)		
C(18)-C(19)-H(19A)	120.8		
C(20)-C(19)-H(19A)	120.8		
C(19)-C(20)-C(28)	119.7(6)		
C(19)-C(20)-C(21)	132.1(6)		
C(28)-C(20)-C(21)	108.2(5)		
C(22)-C(21)-C(26)	119.6(6)		
C(22)-C(21)-C(20)	131.3(6)		
C(26)-C(21)-C(20)	109.1(5)		
C(21)-C(22)-C(23)	118.1(6)		
C(21)-C(22)-H(22A)	121.0		
C(23)-C(22)-H(22A)	121.0		
C(24)-C(23)-C(22)	121.4(6)		
C(24)-C(23)-H(23A)	119.3		
C(22)-C(23)-H(23A)	119.3		
C(23)-C(24)-C(25)	120.4(7)		
C(23)-C(24)-C(30)	120.6(7)		
C(25)-C(24)-C(30)	118.9(7)		
C(26)-C(25)-C(24)	117.8(6)		
C(26)-C(25)-H(25A)	121.1		
C(24)-C(25)-H(25A)	121.1		
C(25)-C(26)-C(21)	122.6(6)		
C(25)-C(26)-C(27)	128.6(6)		
C(21)-C(26)-C(27)	108.8(5)		
O(6)-C(27)-C(28)	127.6(6)		
O(6)-C(27)-C(26)	126.9(6)		
C(28)-C(27)-C(26)	105.4(5)		
C(16)-C(28)-C(20)	122.1(6)		
C(16)-C(28)-C(27)	129.5(6)		

Table 16 Continued: Bond Angles [°] for BaFDC.

	Angle	Symm. op. atom 1	Symm. op. atom 3
C(20)-C(28)-C(27)	108.4(5)		
O(8)-C(29)-O(7)	123.2(9)		
O(8)-C(29)-C(17)	118.0(8)		
O(7)-C(29)-C(17)	118.8(9)		
O(8)-C(29)-Ba(1)	57.4(5)		
O(7)-C(29)-Ba(1)	70.8(5)		
C(17)-C(29)-Ba(1)	155.5(6)		
O(9)-C(30)-O(10)	125.4(9)		
O(9)-C(30)-C(24)	117.7(8)		
O(10)-C(30)-C(24)	116.8(8)		
Ba(1)-O(11)-H(11A)	109(9)		
Ba(1)-O(11)-H(11B)	139(10)		
H(11A)-O(11)-H(11B)	82(4)		
Ba(2)-O(12)-H(12A)	134(6)		
Ba(2)-O(12)-H(12B)	138(5)		
H(12A)-O(12)-H(12B)	86(4)		
C(10)-C(11)-C(6)	121.9(6)		
C(10)-C(11)-C(12)	129.1(6)		
C(6)-C(11)-C(12)	108.9(5)		
O(1)-C(12)-C(11)	127.7(6)		
O(1)-C(12)-C(13)	127.1(6)		
C(11)-C(12)-C(13)	105.1(5)		
C(1)-C(13)-C(5)	122.3(6)		
C(1)-C(13)-C(12)	129.6(6)		
C(5)-C(13)-C(12)	108.2(5)		
O(2)-C(14)-O(3)	121.6(8)		

4.5 CdFDC structure details
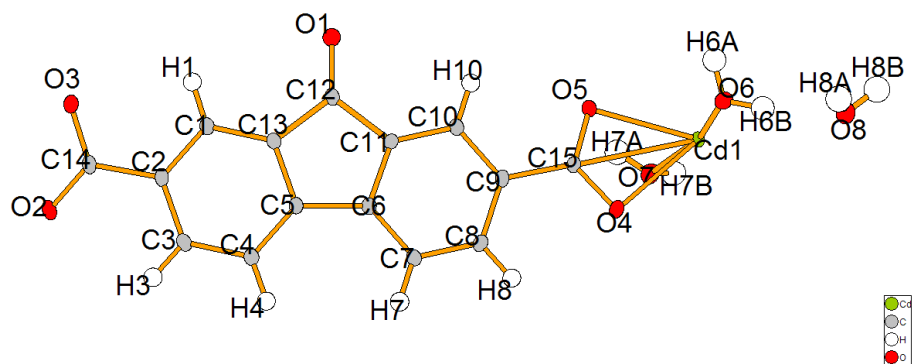
Figure 39 Asymmetric unit with atom numbers for CdFDC.

Table 17 Crystal data and structure refinement for CdFDC.

Parameter	Value
Empirical formula	$C_{15}H_12O_8Cd$
Formula weight	$432.65\,g\cdot mol^{-1}$
Collection Temperature	100(2) K
Wavelength	0.77490Å
Crystal system	Monoclinic
Space Group	$P2(1)/c$
Unit cell dimensions	
a	7.7123(2) Å
b	28.5057(8)Å
c	6.6459(2) Å
α	$90°$
β	$105.050(2)°$
γ	$90°$
Volume	$1410.95(7)Å^3$
Z	4
Calculated density	$2.037\,g/m^3$
Absorption coefficient	$1.982\,mm^{-1}$
F(000)	856
Crystal size	$0.18{\times}0.08{\times}0.03$ mm
Theta range for data collection	$3.08°$ to $33.61°$
Limiting indices	$-11 \leq h \leq 10,\ -39 \leq k \leq 40, -9 \leq l \leq 9$
Reflections collected / unique	20326 / 4304 [R(int) = 0.0523]
Data Completeness	99.7%
Absorption correction	Semi-empirical from equivalents
Max. and min. transmission	0.90 and 0.68
Refinement method	Full-matrix least-squares on F^2
Data / restraints / parameters	4304 / 15 / 235
Goodness-of-fit on F^2	1.045
Final R indices [I>2sigma(I)]	R1 = 0.0257, wR2 = 0.0676
R indices (all data)	R1 = 0.0288, wR2 = 0.0695
Extinction coefficient	0
Largest diff. peak and hole	0.594 and $-0.486\,e\cdot Å^{-3}$

Table 18 Crystal coordinates [Å] and equivalent isotropic displacement parameters [Å^2] for CdFDC. U$_{eq}$ is defined as one third of the trace of the orthogonalized U$_{ij}$ tensor.

	x	y	z	U$_{eq}$
Cd(1)	0.783610(16)	0.523252(4)	0.330768(19)	0.01055(5)
C(1)	0.4144(2)	0.18545(6)	0.3702(3)	0.0117(3)
H(1)	0.2871	0.1837	0.3295	0.014
C(2)	0.5192(2)	0.14461(6)	0.3966(3)	0.0116(3)
C(3)	0.7070(2)	0.14768(6)	0.4595(3)	0.0122(3)
H(3)	0.7765	0.1197	0.4770	0.015
C(4)	0.7940(2)	0.19101(6)	0.4970(3)	0.0119(3)
H(4)	0.9212	0.1928	0.5421	0.014
C(5)	0.6901(2)	0.23129(6)	0.4669(3)	0.0104(3)
C(6)	0.7429(2)	0.28140(6)	0.4818(3)	0.0107(3)
C(7)	0.9104(2)	0.30256(6)	0.5306(3)	0.0126(3)
H(7)	1.0169	0.2843	0.5681	0.015
C(8)	0.9189(2)	0.35164(6)	0.5234(3)	0.0119(3)
H(8)	1.0327	0.3667	0.5566	0.014
C(9)	0.7631(2)	0.37889(6)	0.4683(3)	0.0111(3)
C(10)	0.5935(2)	0.35724(6)	0.4205(3)	0.0117(3)
H(10)	0.4868	0.3755	0.3837	0.014
C(11)	0.5853(2)	0.30889(6)	0.4282(3)	0.0106(3)
C(12)	0.4259(2)	0.27692(6)	0.3771(3)	0.0119(3)
O(1)	0.26768(18)	0.28792(5)	0.3192(2)	0.0171(3)
C(13)	0.5016(2)	0.22843(6)	0.4049(3)	0.0108(3)
C(14)	0.4301(3)	0.09775(6)	0.3430(3)	0.0123(3)
O(2)	0.51881(19)	0.06241(5)	0.3188(2)	0.0163(3)
O(3)	0.25901(18)	0.09631(5)	0.3130(2)	0.0149(3)
C(15)	0.7735(2)	0.43118(6)	0.4434(3)	0.0106(3)
O(4)	0.92334(18)	0.45208(5)	0.4995(2)	0.0150(3)
O(5)	0.63122(18)	0.45317(4)	0.3552(2)	0.0135(2)
O(6)	0.72896(18)	0.54311(5)	0.6454(2)	0.0154(3)
H(6A)	0.6174(19)	0.5440(10)	0.633(4)	0.023
H(6B)	0.780(4)	0.5679(7)	0.700(4)	0.023
O(7)	0.8136(2)	0.48861(5)	0.0282(2)	0.0171(3)
H(7A)	0.729(3)	0.4705(8)	-0.029(4)	0.026
H(7B)	0.819(4)	0.5063(9)	-0.071(4)	0.026
O(8)	0.8619(2)	0.62203(5)	0.8435(2)	0.0195(3)
H(8A)	0.831(4)	0.6181(10)	0.956(3)	0.029
H(8B)	0.819(4)	0.6485(6)	0.798(4)	0.029

Table 19 Anisotropic displacement parameters [Å^2] for CdFDC. The anisotropic displacement factor exponent takes the form $-2\pi^2[h^2a^{*2}U^{11} + ... + 2hka^*b^*U^{12}]$.

	U^{11}	U^{22}	U^{33}	U^{23}	U^{13}	U^{12}
Cd(1)	0.01018(8)	0.00669(8)	0.01377(8)	0.00134(4)	0.00129(5)	0.00008(4)
C(1)	0.0122(8)	0.0089(7)	0.0130(8)	-0.0004(6)	0.0012(6)	-0.0002(6)
C(2)	0.0141(8)	0.0079(7)	0.0124(7)	-0.0006(6)	0.0025(6)	-0.0013(6)
C(3)	0.0138(8)	0.0090(7)	0.0128(7)	-0.0004(6)	0.0018(6)	0.0014(6)
C(4)	0.0121(8)	0.0095(7)	0.0134(8)	0.0000(6)	0.0020(6)	0.0000(6)
C(5)	0.0113(8)	0.0086(7)	0.0108(7)	0.0001(5)	0.0019(6)	-0.0008(6)
C(6)	0.0123(8)	0.0090(7)	0.0106(7)	0.0002(6)	0.0023(6)	-0.0003(6)
C(7)	0.0117(8)	0.0093(7)	0.0158(8)	-0.0001(6)	0.0015(6)	0.0007(6)
C(8)	0.0106(8)	0.0110(8)	0.0136(8)	-0.0009(6)	0.0024(6)	-0.0023(6)
C(9)	0.0125(8)	0.0086(7)	0.0116(7)	0.0000(6)	0.0024(6)	-0.0019(6)
C(10)	0.0121(8)	0.0090(7)	0.0141(8)	0.0001(6)	0.0036(6)	0.0001(6)
C(11)	0.0093(7)	0.0094(7)	0.0129(7)	-0.0008(6)	0.0025(6)	-0.0011(6)
C(12)	0.0125(8)	0.0089(7)	0.0140(8)	0.0001(6)	0.0030(6)	0.0000(6)
O(1)	0.0134(7)	0.0133(7)	0.0240(7)	0.0011(5)	0.0036(5)	0.0000(5)
C(13)	0.0113(8)	0.0086(7)	0.0119(7)	0.0000(5)	0.0021(6)	0.0004(6)
C(14)	0.0159(8)	0.0085(7)	0.0109(7)	0.0001(6)	0.0005(6)	-0.0008(6)
O(2)	0.0175(7)	0.0085(6)	0.0214(7)	-0.0029(5)	0.0022(5)	0.0004(5)
O(3)	0.0133(6)	0.0099(6)	0.0195(7)	-0.0020(5)	0.0007(5)	-0.0017(5)
C(15)	0.0119(8)	0.0089(7)	0.0108(7)	0.0009(6)	0.0027(6)	-0.0012(6)
O(4)	0.0121(6)	0.0101(6)	0.0212(7)	0.0012(5)	0.0011(5)	-0.0024(5)
O(5)	0.0118(6)	0.0088(6)	0.0193(6)	0.0030(5)	0.0029(5)	0.0004(4)
O(6)	0.0125(6)	0.0152(7)	0.0188(7)	-0.0020(5)	0.0042(5)	-0.0016(5)
O(7)	0.0176(7)	0.0162(6)	0.0175(7)	-0.0015(5)	0.0045(5)	-0.0034(5)
O(8)	0.0203(7)	0.0160(7)	0.0221(7)	-0.0003(5)	0.0054(6)	-0.0015(5)

Table 20 Symmetry operations used in the following tables for CdFDC.

	Operation
#1	'x,y,z'
#2	'-x,y+1/2,-z+1/2'
#3	'-x,-y,-z'
#4	'x,-y-1/2,z-1/2'

Table 21 Bond Lengths [Å] for CdFDC.

	Angle	Symm. op. atom 1	Symm. op. atom 3
Cd(1)-O(7)	2.3050(15)		
Cd(1)-O(6)	2.3080(14)		
Cd(1)-O(5)	2.3447(13)		
Cd(1)-O(4)	2.3561(14)	3	
Cd(1)-O(4)	2.4305(13)		
Cd(1)-O(2)	2.5437(14)	2	
Cd(1)-C(15)	2.7357(17)		
Cd(1)-C(14)	2.7516(18)	2	
C(1)-C(13)	1.388(2)		
C(1)-C(2)	1.402(2)		
C(1)-H(1)	0.9500		
C(2)-C(3)	1.402(2)		
C(2)-C(14)	1.502(2)		
C(3)-C(4)	1.397(2)		
C(3)-H(3)	0.9500		
C(4)-C(5)	1.385(2)		
C(4)-H(4)	0.9500		
C(5)-C(13)	1.407(2)		
C(5)-C(6)	1.481(2)		
C(6)-C(7)	1.386(2)		
C(6)-C(11)	1.412(2)		
C(7)-C(8)	1.402(2)		
C(7)-H(7)	0.9500		
C(8)-C(9)	1.397(2)		
C(8)-H(8)	0.9500		
C(9)-C(10)	1.406(2)		
C(9)-C(15)	1.504(2)		
C(10)-C(11)	1.381(2)		
C(10)-H(10)	0.9500		
C(11)-C(12)	1.496(2)		
C(12)-O(1)	1.221(2)		
C(12)-C(13)	1.493(2)		
C(14)-O(2)	1.251(2)		
C(14)-O(3)	1.283(2)		
C(14)-Cd(1)	2.7515(18)	2	
O(2)-Cd(1)	2.5436(14)	2	
O(3)-Cd(1)	2.2792(14)	2	
C(15)-O(4)	1.267(2)		
C(15)-O(5)	1.267(2)		
O(4)-Cd(1)	2.3561(13)	3	
O(6)-H(6A)	0.844(13)		
O(6)-H(6B)	0.845(13)		
O(7)-H(7A)	0.843(13)		
O(7)-H(7B)	0.839(13)		
O(8)-H(8A)	0.845(13)		
O(8)-H(8B)	0.848(13)		

Table 22 Bond Angles [°] for CdFDC.

	Angle	Symm. op. atom 1	Symm. op. atom 3
O(7)-Cd(1)-O(5)	82.02(5)		
O(6)-Cd(1)-O(5)	86.19(5)		
O(3)-Cd(1)-O(4)	86.79(5)	2	3
O(7)-Cd(1)-O(4)	104.15(5)		3
O(6)-Cd(1)-O(4)	82.59(5)		3
O(5)-Cd(1)-O(4)	131.06(5)		3
O(3)-Cd(1)-O(4)	162.65(5)	2	
O(7)-Cd(1)-O(4)	84.94(5)		
O(6)-Cd(1)-O(4)	87.15(5)		
O(5)-Cd(1)-O(4)	55.04(4)		
O(4)-Cd(1)-O(4)	76.88(5)	3	
O(3)-Cd(1)-O(2)	54.37(5)	2	2
O(7)-Cd(1)-O(2)	97.87(5)		2
O(6)-Cd(1)-O(2)	83.20(5)		2
O(5)-Cd(1)-O(2)	88.61(4)		2
O(4)-Cd(1)-O(2)	136.41(4)	3	2
O(4)-Cd(1)-O(2)	142.97(5)		2
O(3)-Cd(1)-C(15)	168.51(5)	2	
O(7)-Cd(1)-C(15)	81.03(5)		
O(6)-Cd(1)-C(15)	87.86(5)		
O(5)-Cd(1)-C(15)	27.54(5)		
O(4)-Cd(1)-C(15)	104.32(5)	3	
O(4)-Cd(1)-C(15)	27.59(5)		
O(2)-Cd(1)-C(15)	116.07(5)	2	
O(3)-Cd(1)-C(14)	27.56(5)	2	2
O(7)-Cd(1)-C(14)	98.60(5)		2
O(6)-Cd(1)-C(14)	87.74(5)		2
O(5)-Cd(1)-C(14)	115.48(5)		2
O(4)-Cd(1)-C(14)	111.48(5)	3	2
O(4)-Cd(1)-C(14)	169.53(5)		2
O(2)-Cd(1)-C(14)	26.97(5)	2	2
C(15)-Cd(1)-C(14)	143.00(5)		2
C(13)-C(1)-C(2)	118.30(16)		
C(13)-C(1)-H(1)	120.9		
C(2)-C(1)-H(1)	120.9		
C(1)-C(2)-C(3)	120.17(16)		
C(1)-C(2)-C(14)	119.71(16)		
C(3)-C(2)-C(14)	119.99(16)		
C(4)-C(3)-C(2)	121.31(16)		
C(4)-C(3)-H(3)	119.3		
C(2)-C(3)-H(3)	119.3		
C(5)-C(4)-C(3)	118.32(17)		
C(5)-C(4)-H(4)	120.8		
C(3)-C(4)-H(4)	120.8		
C(4)-C(5)-C(13)	120.62(16)		
C(4)-C(5)-C(6)	130.65(16)		
C(13)-C(5)-C(6)	108.69(15)		
C(7)-C(6)-C(11)	120.45(16)		
C(7)-C(6)-C(5)	131.17(16)		
C(11)-C(6)-C(5)	108.34(15)		
C(6)-C(7)-C(8)	118.36(16)		
C(6)-C(7)-H(7)	120.8		
C(8)-C(7)-H(7)	120.8		
C(9)-C(8)-C(7)	121.28(16)		
C(9)-C(8)-H(8)	119.4		
C(7)-C(8)-H(8)	119.4		
C(8)-C(9)-C(10)	120.09(16)		
C(8)-C(9)-C(15)	120.85(15)		
C(10)-C(9)-C(15)	118.90(16)		
C(11)-C(10)-C(9)	118.58(16)		

Table 23 Continued: Bond Angles [°] for CdFDC.

|	Angle	Symm. op. atom 1	Symm. op. atom 3
C(11)-C(10)-H(10)	120.7		
C(9)-C(10)-H(10)	120.7		
C(10)-C(11)-C(6)	121.22(16)		
C(10)-C(11)-C(12)	129.94(16)		
C(6)-C(11)-C(12)	108.78(15)		
O(1)-C(12)-C(13)	127.09(17)		
O(1)-C(12)-C(11)	127.57(16)		
C(13)-C(12)-C(11)	105.31(15)		
C(1)-C(13)-C(5)	121.26(16)		
C(1)-C(13)-C(12)	129.80(16)		
C(5)-C(13)-C(12)	108.87(15)		
O(2)-C(14)-O(3)	121.94(17)		
O(2)-C(14)-C(2)	120.97(17)		
O(3)-C(14)-C(2)	116.99(16)		
O(2)-C(14)-Cd(1)	67.22(10)		2
O(3)-C(14)-Cd(1)	55.27(9)		2
C(2)-C(14)-Cd(1)	166.68(12)		2
C(14)-O(2)-Cd(1)	85.81(11)		2
C(14)-O(3)-Cd(1)	97.17(11)		2
O(4)-C(15)-O(5)	121.17(16)		
O(4)-C(15)-C(9)	120.28(16)		
O(5)-C(15)-C(9)	118.44(15)		
O(4)-C(15)-Cd(1)	62.67(9)		
O(5)-C(15)-Cd(1)	58.79(9)		
C(9)-C(15)-Cd(1)	170.71(12)		
C(15)-O(4)-Cd(1)	165.79(12)		3
C(15)-O(4)-Cd(1)	89.74(10)		
Cd(1)-O(4)-Cd(1)	103.12(5)	3	
C(15)-O(5)-Cd(1)	93.67(11)		
Cd(1)-O(6)-H(6A)	110.1(19)		
Cd(1)-O(6)-H(6B)	114.8(19)		
H(6A)-O(6)-H(6B)	112(3)		
Cd(1)-O(7)-H(7A)	114(2)		
Cd(1)-O(7)-H(7B)	118(2)		
H(7A)-O(7)-H(7B)	102(3)		
H(8A)-O(8)-H(8B)	105(3)		

4.6   MnFDC structure details
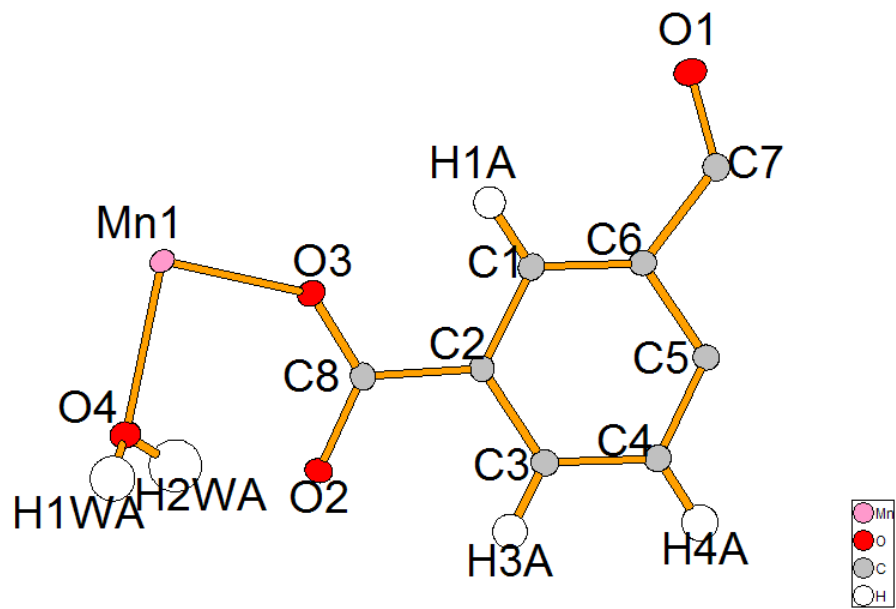
Figure 40 Asymmetric unit with atom numbers for MnFDC.

Table 24 Crystal data and structure refinement for MnFDC.

Parameter	Value
Empirical formula	$C_{15}H_{10}O_7Mn$
Formula weight	$357.17\,g\cdot mol^{-1}$
Collection Temperature	100(2) K
Wavelength	0.77490Å
Crystal system	Monoclinic
Space Group	$C2/c$
Unit cell dimensions	
a	26.943(2)Å
b	7.2476(6)Å
c	6.9261(5)Å
α	90°
β	97.703(2)°
γ	90°
Volume	1340.27Å^3
Z	4
Calculated density	1.770 g/m^3
Absorption coefficient	1.287 mm^{-1}
F(000)	724
Crystal size	0.11×0.03×0.01 mm
Theta range for data collection	3.95° to 33.60°
Limiting indices	$-38 \leq h \leq 38, 0 \leq k \leq 10, 0 \leq l \leq 9$
Reflections collected / unique	14469 / 2016 [R(int) = 0.0351]
Data Completeness	99.2%
Absorption correction	Semi-empirical from equivalents
Max. and min. transmission	0.93 and 0.84
Refinement method	Full-matrix least-squares on F^2
Data / restraints / parameters	2016 / 0 / 116
Goodness-of-fit on F^2	1.045
Final R indices [I>2sigma(I)]	R1 = 0.0258, wR2 = 0.0631
R indices (all data)	R1 = 0.0312, wR2 = 0.0660
Extinction coefficient	0
Largest diff. peak and hole	0.502 and -0.290$e\cdot$Å^{-3}

Table 25 Crystal coordinates [Å] and equivalent isotropic displacement parameters [Å^2] for MnFDC. U$_{eq}$ is defined as one third of the trace of the orthogonalized U$_{ij}$ tensor.

	x	y	z	U$_{eq}$
Mn(1)	0.2500	0.7500	0.0000	0.01056(8)
O(1)	0.0000	0.8255(2)	0.2500	0.0243(4)
O(2)	0.21209(4)	0.33697(13)	0.21582(17)	0.01266(19)
O(3)	0.19208(4)	0.63223(14)	0.14824(16)	0.0142(2)
C(1)	0.09294(5)	0.57709(19)	0.2192(2)	0.0132(3)
H(1A)	0.1034	0.7017	0.2112	0.016
C(2)	0.12705(5)	0.43129(18)	0.2148(2)	0.0121(2)
C(3)	0.11108(5)	0.24814(19)	0.2289(2)	0.0158(3)
H(3A)	0.1348	0.1512	0.2301	0.019
C(4)	0.06095(5)	0.2049(2)	0.2411(3)	0.0171(3)
H(4A)	0.0503	0.0804	0.2476	0.021
C(5)	0.02732(5)	0.34959(19)	0.2433(2)	0.0137(3)
C(6)	0.04362(5)	0.53403(18)	0.2356(2)	0.0131(3)
C(7)	0.0000	0.6581(3)	0.2500	0.0145(4)
C(8)	0.18054(5)	0.47134(18)	0.1920(2)	0.0111(2)
O(4)	0.28846(4)	0.48028(14)	0.03761(19)	0.0150(2)
H(1WA)	0.2971(8)	0.413(3)	-0.048(4)	0.032(6)
H(2WA)	0.2719(9)	0.408(4)	0.104(4)	0.044(7)

Table 26 Anisotropic displacement parameters [Å^2] for MnFDC. The anisotropic displacement factor exponent takes the form $-2\pi^2[h^2a^{*2}U^{11} + ... + 2hka^*b^*U^{12}]$.

	U^{11}	U^{22}	U^{33}	U^{23}	U^{13}	U^{12}
Mn(1)	0.01050(12)	0.00762(12)	0.01372(13)	-0.00029(10)	0.00218(12)	-0.00109(10)
O(1)	0.0183(7)	0.0113(7)	0.0441(11)	0.000	0.0069(7)	0.000
O(2)	0.0116(4)	0.0101(4)	0.0162(5)	0.0012(4)	0.0020(4)	0.0017(3)
O(3)	0.0132(4)	0.0102(4)	0.0197(5)	0.0012(4)	0.0046(4)	-0.0009(4)
C(1)	0.0117(6)	0.0111(5)	0.0169(7)	0.0011(5)	0.0022(5)	-0.0008(5)
C(2)	0.0096(5)	0.0120(5)	0.0149(7)	0.0010(5)	0.0017(5)	-0.0002(5)
C(3)	0.0123(6)	0.0113(6)	0.0241(8)	0.0012(5)	0.0036(5)	0.0008(5)
C(4)	0.0121(6)	0.0112(5)	0.0284(8)	0.0018(5)	0.0039(5)	-0.0001(5)
C(5)	0.0116(6)	0.0114(6)	0.0185(7)	-0.0001(5)	0.0032(5)	0.0003(5)
C(6)	0.0121(6)	0.0101(6)	0.0172(7)	0.0006(5)	0.0022(5)	0.0005(5)
C(7)	0.0115(8)	0.0122(8)	0.0195(10)	0.000	0.0013(7)	0.000
C(8)	0.0101(5)	0.0122(6)	0.0110(6)	-0.0007(5)	0.0018(5)	-0.0002(4)
O(4)	0.0163(4)	0.0111(4)	0.0184(6)	0.0000(4)	0.0053(5)	0.0001(4)

Table 27 Symmetry operations used in the following tables for MnFDC.

	Operation
#1	'x,y,z'
#2	'-x,y,-z+1/2'
#3	'x+1/2,y+1/2,z'
#4	'-x+1/2,y+1/2,-z+1/2'
#5	'-x,-y,-z'
#6	'x,-y,z-1/2'
#7	'-x+1/2,-y+1/2,-z'
#8	'x+1/2,-y+1/2,z-1/2'

Table 28 Bond Lengths [Å] for MnFDC.

	Angle	Symm. op. atom 1	Symm. op. atom 3
Mn(1)-O(2)	2.1853(11)	4	
Mn(1)-O(3)	2.1557(10)		
Mn(1)-O(3)	2.1557(10)	7	
Mn(1)-O(4)	2.2114(10)		
Mn(1)-O(4)	2.2114(10)	7	
O(1)-C(7)	1.213(3)		
O(2)-Mn(1)	2.1853(11)	4	
O(2)-C(8)	1.2888(15)		
O(3)-C(8)	1.2544(16)		
C(1)-H(1A)	0.9500		
C(1)-C(2)	1.4034(18)		
C(1)-C(6)	1.3845(18)		
C(2)-C(3)	1.4028(18)		
C(2)-C(8)	1.4990(18)		
C(3)-H(3A)	0.9500		
C(3)-C(4)	1.3999(19)		
C(4)-H(4A)	0.9500		
C(4)-C(5)	1.387(2)		
C(5)-C(5)	1.487(3)	2	
C(5)-C(6)	1.4103(19)		
C(6)-C(7)	1.4938(18)		
C(7)-C(6)	1.4937(18)	2	
O(4)-H(1WA)	0.82(3)		
O(4)-H(2WA)	0.86(3)		

Table 29 Bond Angles [°] for MnFDC.

	Angle	Symm. op. atom 1	Symm. op. atom 3
O(2)-Mn(1)-O(3)	91.95(4)	4	7
O(2)-Mn(1)-O(4)	89.65(4)	6	7
O(2)-Mn(1)-O(4)	90.35(4)	4	7
O(2)-Mn(1)-O(4)	90.35(4)	6	
O(2)-Mn(1)-O(4)	89.65(4)	4	
O(3)-Mn(1)-O(3)	180.0		7
O(3)-Mn(1)-O(4)	87.22(4)		
O(3)-Mn(1)-O(4)	92.78(4)		7
O(3)-Mn(1)-O(4)	87.22(4)	7	7
O(3)-Mn(1)-O(4)	92.78(4)	7	
O(4)-Mn(1)-O(4)	180.00(5)		7
Mn(1)-O(2)-C(8)	123.64(9)	4	
Mn(1)-O(3)-C(8)	134.58(9)		
H(1A)-C(1)-C(2)	121.0		
H(1A)-C(1)-C(6)	121.0		
C(2)-C(1)-C(6)	118.07(12)		
C(1)-C(2)-C(3)	120.20(12)		
C(1)-C(2)-C(8)	119.87(12)		
C(3)-C(2)-C(8)	119.92(12)		
C(2)-C(3)-H(3A)	119.2		
C(2)-C(3)-C(4)	121.56(13)		
H(3A)-C(3)-C(4)	119.2		
C(3)-C(4)-H(4A)	121.0		
C(3)-C(4)-C(5)	117.93(13)		
H(4A)-C(4)-C(5)	121.0		
C(4)-C(5)-C(5)	130.85(8)		2
C(4)-C(5)-C(6)	120.59(13)		
C(5)-C(5)-C(6)	108.55(8)	2	
C(1)-C(6)-C(5)	121.60(13)		
C(1)-C(6)-C(7)	129.95(12)		
C(5)-C(6)-C(7)	108.45(12)		
O(1)-C(7)-C(6)	127.02(8)		
O(1)-C(7)-C(6)	127.02(8)		2
C(6)-C(7)-C(6)	105.96(16)		2
O(2)-C(8)-O(3)	123.55(12)		
O(2)-C(8)-C(2)	117.85(12)		
O(3)-C(8)-C(2)	118.59(12)		
Mn(1)-O(4)-H(1WA)	127.6(17)		
Mn(1)-O(4)-H(2WA)	109.5(17)		
H(1WA)-O(4)-H(2WA)	104(2)		

References

[1] J. C. Lashley, M. F. Hundley, A. Migliori, J. L. Sarrao, P. G. Pagliuso, T. W. Darling, M. Jaime, J. C. Cooley, W. L. Hults, L. Morales, D. J. Thoma, J. L. Smith, J. Boerio-Goates, B. F. Woodfield, G. R. Stewart, R. A. Fisher, and N. E. Phillips. Critical examination of heat capacity measurements made on a quantum design physical property measurement system. *Cryogenics*, 43(6):369–378, 2003.

[2] B. C. Melot, R. Tackett, J. O'Brien, A. L. Hector, G. Lawes, R. Seshadri, and A. P. Ramirez. Large low-temperature specific heat in pyrochlore $Bi_2Ti_2O_7$. *Phys. Rev. B*, 79:224111, 2009.

[3] C. Kittel and H. Kroemer. *Thermal Physics*. W. H. Freeman, New York, 2nd edition, 1980.

[4] D. R. Gaskell. *Introduction to the thermodynamics of materials*. Taylor and Francis, New York, 4th edition, 2003.

[5] A. Tari. *The specific heat of matter at low temperatures*. Imperial College Press, London, 2003.

[6] M. A. Ramos, S. Vieira, F. J. Bermejo, J. Dawidowski, H. E. Fischer, H. Schober, M. A. González andn C. K. Loong, and D. L. Price. Quantitative assessment of the effects of orientational and positional disorder on glassy dynamics. *Phys. Rev. Lett.*, 78:82–85, 1997.

[7] N.C. Greenham, I.D.W. Samuel, G.R. Hayes, R.T. Phillips, Y.A.R.R. Kessener, S.C. Moratti, A.B. Holmes, and R.H. Friend. Measurement of absolute photoluminescence quantum efficiencies in conjugated polymers. *Chem. Phys. Lett.*, 241:89, 1995.

[8] W. Becker. *Advanced Time-Correlated Single Photon Counting Techniques*. Springer-Verlag, New York, 2005.

[9] S. Zhou, Z. Fu, J. Zhang, and S. Zhang. Spectral properties of rare-earth ions in nanocrystalline YAG:Re (Re=Ce^{3+}, Pr^{3+}, Tb^{3+}). *J. Lumines.*, 118:179–185, 2006.

[10] J. D. Furman, G. Gundiah, K. Page, N. Pizarro, and A. K. Cheetham. Local structure and time resolved luminescence of emulsion prepared YAG nanoparticles. *Chem. Phys. Lett.*, 465:67–72, 2008.

[11] Bruker. SAINT Frame Integration Software, Bruker AXS Inc., 2000.

[12] G. M. Sheldrick. *SADABS User Guide*. University of Göttingen, Göttingen, Germany, 1995.

[13] G. M. Sheldrick. *Cell_Now*. Bruker-AXS, Inc., Madison, WI, 2004.

[14] J. D. Furman, A. Y. Warner, S. J. Teat, A. A. Mikhailovsky, and A. K. Cheetham. Tunable, ligand-based emission from inorganicorganic frameworks: A new approach to phosphors for solid state lighting and other applications. *Chem. Mater.*, 22:2255–2260, 2010.

[15] A. K. Cheetham, C. N. R. Rao, and R. K. Feller. Structural diversity and chemical trends in hybrid inorganic-organic framework materials. *Chem. Commun.*, 46:4780–4795, 2006.